Student thesis series INES nr 308

Urban Heat Island in Erbil City

Nazar Jameel Khalid

2014

Department of

Physical Geography and Ecosystems Science

Lund University

Sölvegatan 12

S-223 62 Lund

Sweden

Nazar Jameel Khalid (2014). Urban Heat Island in Erbil City.

Master degree thesis, 30 credits in *Physical geography* Ecosystem Analysis

Department of Physical Geography and Ecosystems Science, Lund University

Seminar series nr 308

Urban Heat Island in Erbil City

Nazar Jameel Khalid

Master thesis, 30 credits, in Physical geography and ecosystem analysis

Supervisor:

Ulrik Mårtensson

Department of Physical Geography and Ecosystem Science

Lund University

March 2014

Abstract

Most cities have been growing and developing at an accelerated rate throughout the world, in both developing and developed countries. Urban growth and development removes the natural land cover and replaces it with a new cover of manmade features (e.g. buildings, streets, industrial areas, commercial complexes etc.). Accordingly, the local climate of these cites has been modified by new land use and land cover alterations which has created the Urban Heat Island (UHI) phenomenon. Erbil City in northern Iraq has been selected as a case study for the effect of urbanization on the local climate of the cities.

Two sets of data were used in this study: ground weather station maximum and minimum air temperature data, over a long period for the city and surrounding rural areas, and satellite image data of the city. The results from the analysis of weather station data revealed significant changes in the local climate of the city over the time series and when comparing the spatial trend of the city with rural stations(mainly for minimum air temperature). The satellite image was used to develop a map of NDVI for the city, which in turn was used to draw the land surface temperature map of Erbil City. From this map there were indications of temperature variations from the thermal reflections of each land use and land cover of the city. The greatest proliferation of hot spots is observed over industrial areas, where the UHI are expected to develop, while the coldest areas comprise green zones.

Key words: Urban heat island, UHI, minimum air temperature, urbanization, urban planning, climate, temperature, Erbil City.

Acknowledgements

I would like to express my great appreciation of my supervisor, Professor Ulrik Martensson, for his constructive and valuable advice, helpful ideas and recommendations to improve my writing and the work of this thesis.

My gratitude to all teachers and staff in the Department of Physical Geography and Ecosystem Analysis for teaching and assisting in Lund University.

Thanks to the friendly and joyful people of Lund in particular and generally to all the people of Sweden for my nice stay.

For supporting me throughout my life, I would also finally like to thank all of my family.

Table of Contents

List of Figures

List of Tables

List of Abbreviations

Ta,max	Mean Maxmum Air Temperature
Ta,min	Mean Minimum Air Temperature
BSh	Semi-arid Climate
CO_2	Carbon Dioxide
Csa	Mediterranean Climate
DN	Digital Number
ETM+	Enhanced Thematic Mapper Plus
GIS	Geographic Information Systems
GMES	Global Monitoring for Environment and Security
IDW	Inverse Distance Weight
LST	Land Surface Temperature
LSE	Land Surface Emissivity
LULC	Land Use, LandCover
NDVI	Normalized Difference Vegetation Index
NOx	Nitrogen Oxides
SUHI	Surface Urban Heat Island
TM	Thematic Mapper
UHI	Urban Heat Island
USGS	United States Geological Survey
UTM	Universal Transverse Mercator

1. Introduction: Background and Literature Review

1.1 The Urban Heat Island (UHI) Phenomenon

Urbanization is the main anthropogenic process responsible for radical changes in the nature of the atmospheric and surface characteristics of a region. The distinctive biophysical features of the urban areas might be expected to be the main causes that amplify the effects of climate change (Figure 1) and cause the climate of urban areas to behave more abnormally (Fortuniak, 2009).

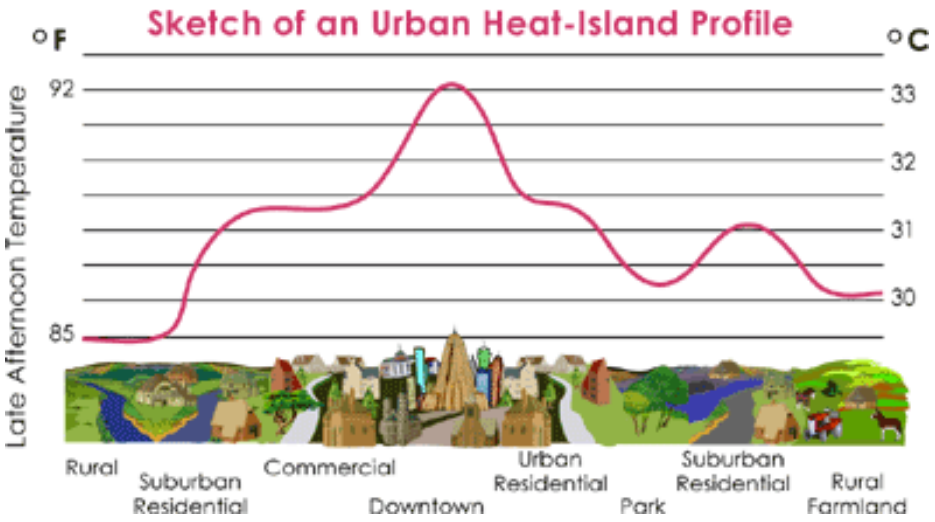

Figure 1: A typical UHI profile (Reproduced from EPA 2009a).

As a consequence of continuous altering of the natural land cover to more man-made patterns, there is a modification of the radiative fluxes, namely change thermal properties of surfaces and trapped fluxes due to multiple reflections. Consequently, the solar radiation and hydrologic balances are dislocated (Figure 2), which in turn increases urban-rural contrast in air temperatures and surface radiance (Brazel et al., 2000). These differences in air temperature between an urban area and its surrounding area are called the Urban Heat Island phenomenon (UHI) (Oke, 1987).

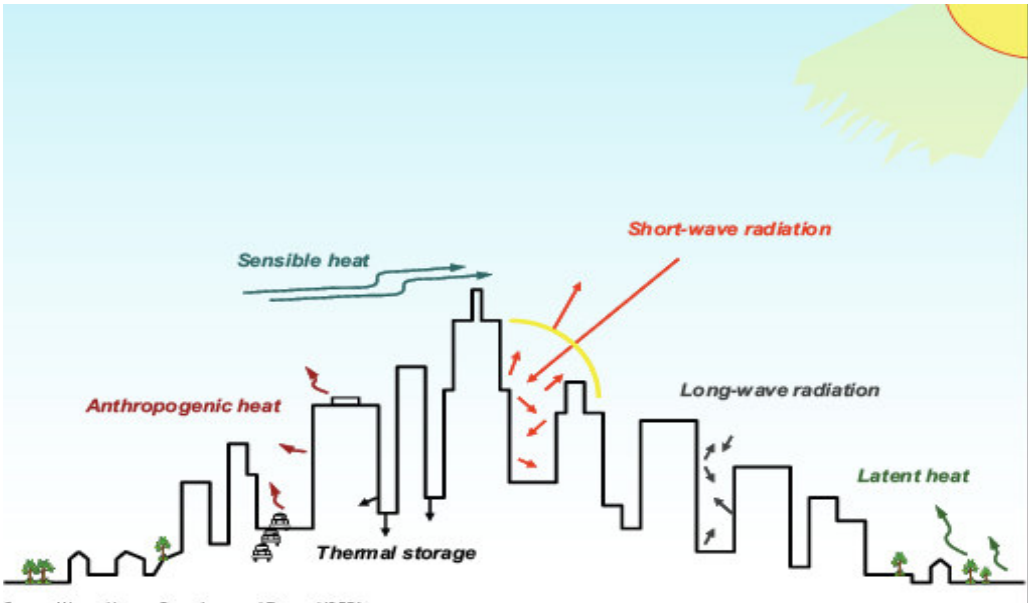

Figure 2: Transformation of thermal heat and radiations inside urban areas (Reproduced from Sailor et al, 2012).

UHI phenomenon has been confirmed by numerous studies to have a role in climatic change in most cities and is considered to be one of climatic phenomena that require more investigation as part of global efforts to address climate change and environmental degradation (Changnon, 1992; Klysik and Fortuniak, 1999; Brazel et al., 2000; Comrie, 2000; Weng, 2003; Serra, 2007; Gaffin et al., 2008).

During daytime at pedestrian level, air temperatures might be lower inside cities than outside it (Johansson, 2006). However, it has been proven in many studies that air temperatures in downtown during the night are generally higher than air temperatures in surrounding rural areas (Meyer, 1991; Oke, 1973; Chapman 2005; Voogt 2004; EPA 2007).

An urban area is often observed to be significantly warmer than those of nearby areas dominated by vegetation, although they have equal exposure to solar energy. The reflection of the solar radiation in urban areas is intensified by the volume of concrete and other man-made materials used for buildings and road construction. These bulks of concrete with their different topographies behave as a good trap for sunlight during the day, and release it into the evening slowly as infrared heat, producing the phenomenon of UHI. Conversely, vegetated areas mostly tend to be covered by trees, It is estimated that a matured tree has a projection area (canopy) of about $50m^2$ (Huang et al, 1987). The $50m^2$ canopy has a high potential to reduce the penetration of solar radiation. These trees absorb the sunlight and releases energy by long-wave emission more readily (Lo et al., 1997; Rose and Devadas, 2009).

Large cities are measured regularly during the nighttime to be about 5 to 10 ℃ warmer than the rural surrounding area (United States Department of Energy, 1996). However, in some cases this temperature discrepancy has been measured to be more than 11℃ (EPA, 2009a).On calm and clear nights the differential cooling rates between urban areas and the rural areas are usually most distinct. Accordingly, UHI acts as a model for climate change researches due to its role in exacerbating the existing heat island phenomenon in urban areas by absorbing increased solar radiation. Furthermore, the climate modifications due to the effect of UHI that have happened in more cities over the second half of the last century are compatible and have the same trend to some extent with the results obtained from models to project the future climate (Karl et al,1988; IPCC,2001).

The magnitude of UHI is called UHI intensity. UHI intensity tends to vary both hourly and seasonally, and is influenced by factors such as local topography, climate region, city size, density, and geometry, industrial development, land use and land cover (LULC) characteristics, the characteristics of the surrounding rural areas, wind speed and vegetation abundance (Stathopoulou et al.,2005; Santana, 2007;Fortuniak, 2009). Cloud cover and incoming solar radiation also affect UHI intensity but with less significance than LULC characteristics and the abundance of urban vegetation (Fortuniak, 2009; Arrau and Pena, 2010).

1.2 Urban Heat Island Types

Surface Urban Heat Islands

Surface UHI is also called remotely sensed UHI because it is usually observed using infrared data that allow retrieving land surface temperatures. Surface urban heat islands are typically present at daytime and nighttime, but tend to be stronger during the night (Oke, 1982). On a sunny and hot summer days, the sun can heat dry, exposed urban surfaces, such as pavements and roofs, to a temperature hotter than the air temperature. Conversely the moist surfaces in rural surroundings remain often close to air temperatures (Berdahl and Bretz, 1997). The average difference in daytime surface temperatures between the urban and rural areas is 5 to 10℃, and the differences in nighttime surface temperatures are typically 10 to 15℃, considered higher than the daytime differences (Voogt and Oke, 2003). Surface UHI varies

seasonally, and is usually greater in summer time, due to changes in the incoming solar radiation and drier weather conditions associated with summer in most regions (Oke, 1987).

Atmospheric Urban Heat Islands

In urban areas the warmer air compared to cooler air in nearby rural areas defines the atmospheric urban heat islands. This heat island was divided into two different types:

Canopy layer Urban Heat Islands:

These exist in the layer of air where people live, usually extending from the ground to below the tops of vegetation and roofs.

Boundary layer Urban Heat Islands:

This layer begins from the rooftop level and extends up to the point where urban landscapes no longer affect the atmosphere. This region typically extends no longer than (1.5 km) from the surface (Oke, 1982).

1.3 Urban Heat Island Formation and Affecting Factors

The formation of UHI is determined by several factors, such as vegetative cover availability, properties of urban materials and geometry as well as the geographical location of cities. Large water bodies or mountainous terrain locate near the cities can influence the general wind patterns, which in turn could influence UHI formation (EPA, 2009a).

Vegetation Cover

Vegetation and open land typically dominate the landscape in most rural areas. However, albedo and emissivity of rural areas are different from those of sealed surfaces. The green cover generally helps to lower the surface temperature by providing shade and also helps to reduce the air temperatures through evapotranspiration (EPA, 2009a). During evapotranspiration, vegetation releases water vapor into surrounding air that contributes in reducing air temperature. Conversely, urban areas are characterized by being covered by impervious and dry surfaces, such as conventional roofs, roads and sidewalks. As a result of city development, more vegetation is removed and replaced by more sealed surfaces (i.e. buildings and paving). Any replacement of vegetation with building leads to less moisture and high surface runoff (Figure3).

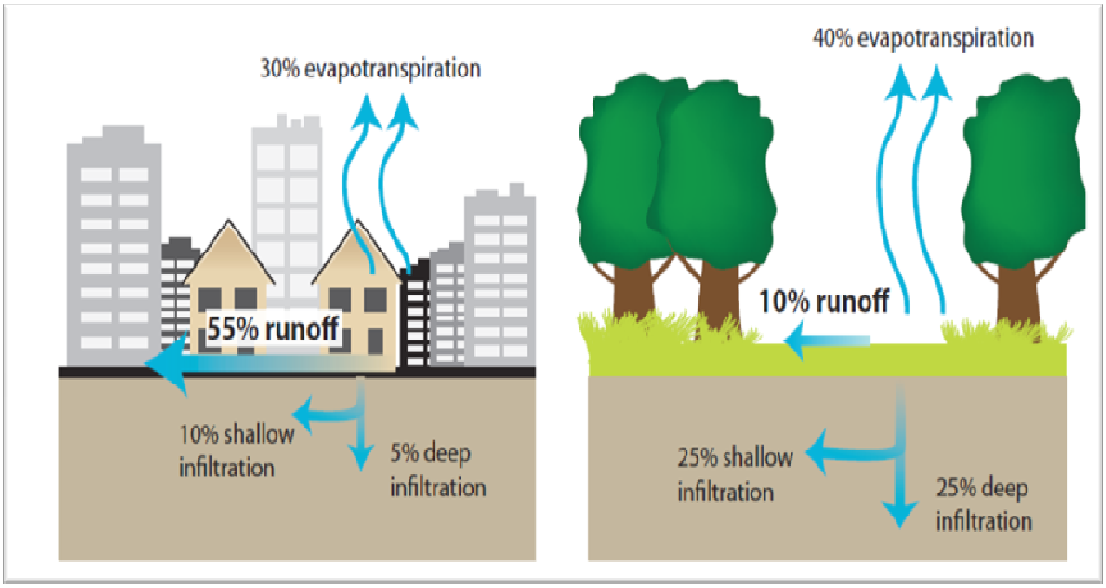

Figure 1: highly developed urban area (left) natural ground cover (right), (Reproduced from EPA, 2009a).

Urban Materials Properties

During the daytime the buildings in the city core absorb and store double the amount of heat of their rural surroundings (EPA, 2009a). Building materials such as stone and steel have higher heat capacity than rural materials, such as dry soil and sand. As a result, the downtown areas in the cities have more efficiency (thermal inertia) than rural surroundings in storing the heat of sun energy inside their infrastructure (Christen and Vogt. 2004).

Solar reflectance, or albedo, is another property that influences heat island development. The highest percentage of solar energy reflected by a surface is found in the visible wavelengths; therefore solar reflectance is correlated with the color of materials. Brighter surfaces tend to have higher reflectance values than darker surfaces.

In case of urban areas, most of their surface materials (such as paved roads and building roofs) have lower effective albedo compared to those in rural areas. Beside the multiple reflections that traps long-wave radiation in the street canyons; consequently built-up areas reflect less and absorb more of the sun's energy (Coutts et al, 2007). The consequence of low effective albedo in urban areas leads to increased surface temperatures and contributes in the formation of surface and atmospheric urban heat islands. The other important factor of materials influencing the formation of UHI is the emissivity.

Surfaces with high emissivity values might stay cooler, due to their higher efficiency in releasing heat (EPA, 2009a).

Urban Geometry

Urban geometry refers to the dimensions and spacing of buildings within a city. Urban geometry influences energy absorption, wind flow, and the surface's ability to emit long-wave radiation back to the sky. The effect of urban geometry is very obvious during the nighttime, since in most developed areas, structures and surfaces are obstructed by objects, such as neighboring buildings; as a result, these areas become a large thermal masses that cannot release their heat readily during the night due to these obstructions (EPA, 2009a). Surface geometry obstructs the sky (due to buildings and related objects) from the urban surface; this effect has been called the sky view factor (SVF) (Figure 4). The surface geometry and surface building materials properties together are considered to be the primary surface controls for most UHIs.

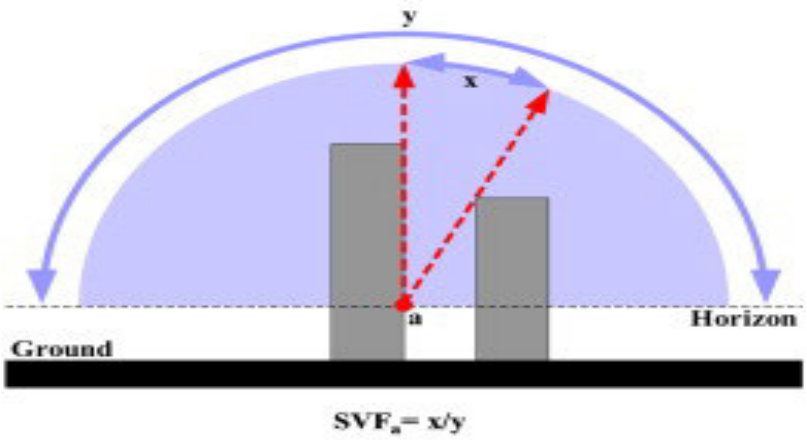

Figure 2: The geometric definition of sky view factor (Reproduced from Zhang et al., 2012).

Where a: the point where the proportions of the sky visible to the overall sky dome.

SVFa = the sky view factor at point a.

X= the radiation emitted by a planar surface.

Y= the radiation emitted by the entire hemispheric environment (Watson and Johnson, 1987).

The reduced SVF of many urban surfaces, particularly those on the ground among buildings, prevent the loss of heat by radiation, due to the cold radiate sky being replaced by relatively

warm surfaces of buildings. Furthermore, reduced surface geometry might provide a sheltering affect that limits convective heat losses. The low values of SVF might limit the energy to enter an area but mostly any reduction in the SVF value is almost always accompanied by increase in UHI intensity (Zhanget al., 2012).

Atmospheric Factors

When wind speeds increase, turbulent mixing exponentially reduces the differences in air temperature near the surface (EPA, 2005a) (Figure 5). Moreover, the atmospheric humidity might reduce the net potential radiative cooling of the surface, therefore high atmospheric humidity is likely increase the heat island intensity (Voogt, 2002). Low humidity areas such as high elevation and desserts locations could generate large air temperature drops. In other words, temperature differences about 40 $^{\circ}$C was measured of the thermally insulated approximate black bodies in the Atacama Desert in Chile (Eriksson and Granqvist, 1982).

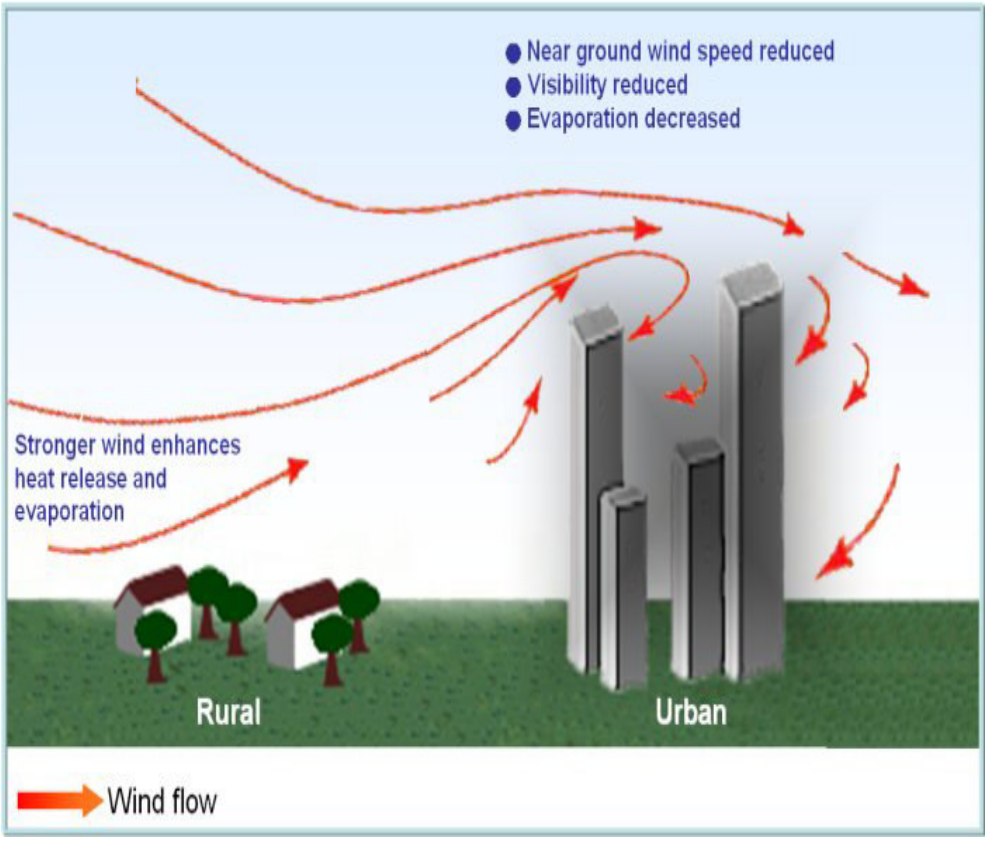

Figure 3: Influence of urban areas on wind flow, and turbulent fluxes of latent and sensible heat, (Reproduced with a Courtesy of the HKO, 2010).

1.4 Impact of the Urban Heat Island

Some positive impacts could result from UHI, such as reductions in energy required for heating, the melting of ice on roads during the winter and lengthening the growing season in the city. Regardless of these positive impacts, the consequences of UHI phenomenon are more perceived on the environment and human health (Akbari, 2005). The most frequent negative impacts in urban areas are:

Energy Consumption

UHI might increase the energy demand for cooling and more pressure to be added to the electricity grid due to most buildings and houses are running cooling systems to reduce the indoor air temperature particularly during extreme heat events. Akbari (2005) found that the electric demand increases 1.5 to 2 percent for every 1°F (0.6°C) increase in summertime temperature in Chicago City. Over the last several decades downtown temperatures have been increasing notably, resulting in a 5 to 10 percent increase in community-wide demand for electricity to compensate the heat island effect (EPA, 2009a).

Fossil Fuel and Air Quality

To accommodate the increased temperature during a dry summer within a city, more energy was consumed by large cities for cooling .Fossil fuels remain the most common source of electricity production worldwide(Chow et al, 2003). The high levels of air pollution and greenhouse gas emissions throughout the world are clearly correlated with the combustion of fossil fuels (Le Treut et al, 2007). Accordingly, pollutants from most power plants form of nitrogen oxides (NOx), sulfur dioxide (SO_2), carbon monoxide (CO), and mercury (Hg). Most of these pollutants are harmful to human health and participate in complex air quality problems such as acid rain (Ed. Hatier, 1993). Fossil-fuel-powered plants participate in global climate change by emitting greenhouse gases, particularly carbon dioxide (CO_2) (EPA, 2009a).

Human Health

The nighttime atmospheric heat islands might lead to serious health implications for urban residents in the case of heat waves (Kalkstein, 1991). Respiratory difficulties, general discomfort, heat cramps and exhaustion, and heat-related mortality are the most common

health problems related to daytime increase of air temperatures and reduction in outdoor nighttime cooling (EPA, 2009a).

Quality of Water

Water quality could be degraded by surface urban heat island through thermal pollutants. High rooftop and pavement surface temperatures could heat storm water runoff. James, (2002) has conducted tests revealed that pavements that are 100°F (38°C) can raise initial rainwater temperature from roughly 70°F (21°C) to over 95ºF (35°C). Accordingly, the heated storm water generally becomes runoff, which drains into storm sewers and elevates water temperatures as it is released into ponds, streams, rivers, and lakes. However, increased run-off temperature could be stressful for aquatic live, for example brook trout experience thermal shock and stress when the water temperature changes in a day by more than (1-2°C) (EPA, 2003).

1.5 Mitigation and Reduction of Urban Heat Island Impacts

Despite the phenomenon of UHI being acknowledged in the literature for decades, concern and community interest regarding the UHI is more recent. The increased attention afforded by climatologists to heat-related environment and health issues has participated in UHI reduction in some cities in the world by the implementation of recommended strategies, for instance promoting trees and vegetation, green roofs and cool roofs(EPA. 2003).

Vegetation and Trees

One major strategy is extensive planting of trees and vegetation. Leaves and branches, participate in cooling the urban area through shading. In late spring and summer time, particularly in mid-latitudes, about 10 to 30 percent of the sun's energy reaches the area below trees, with the remainder either reflected back into the atmosphere or absorbed by leaves and used for photosynthesis (Huang, Akbari and Taha, 1990).

Green Roofs

This technique involves growing a vegetative layer on a conventional rooftop. Green roofs act as trees and vegetation elsewhere; they shade surfaces and remove heat from the air through evapotranspiration. Regardless of rooftop moisture content, they also change the albedo to a

certain extent. The surface of a vegetated rooftop can participate in cooling the ambient air, particularly on hot days, during daytime (Vandermeulen, 2011; Liu and Baskaran, 2003).

Cool Roofs

Cool roof technology employs highly reflective and emissive materials. Cool roof products are in most cases bright and white. These products obtain a high reflectance primarily by reflecting the visible portion of the spectrum. Conventional roofing materials have low solar reflectance of 5 to 15 percent, which means they absorb 85 to 95 percent of the energy that reach them, instead of reflecting the energy back to the atmosphere. Conversely, cool roof materials have high solar reflectance that can exceed 65 percent; therefore they absorb and transfer to buildings less than 35 percent of the energy that reaches them. Furthermore, these materials reflect radiation across the entire solar spectrum, particularly in the infrared and visible wavelengths (EPA, 2009a).

Emissivity or thermal emittance is a very important consideration when selecting materials for installing a cool roof. Any surface exposed to radiant energy become hotter until it reaches thermal equilibrium; in other words it gives off as much heat as it receives. In order to know how much heat the material radiates per unit area at a given temperature, there is a need to know beforehand the material's thermal emissivity. The high-emittance surface gives off its heat more readily because of the surfaces with high emittance reach thermal equilibrium at a lower temperature than surfaces with low emittance (Akbari and Taha, 2003; Rose, 2005).

1.6 Objectives

Effects of climate change are expected to be amplified in urban areas due to their distinctive biophysical features, which are manifested in the UHI phenomenon (Fortuniak, 2009). Therefore, the overall aim of this research was to illustrate the influence of urban growth on the air temperature trend in Erbil City.

Erbil City, the capital of the Kurdistan Region in Iraq, has been selected as study area and this study addresses the following objectives:

1 - To find out if there is an increase in the minimum air temperature (mainly minimum temperature) in Erbil City for the period 1975-2011.

2 - To compare the air temperature inside the city to the air temperature of the surrounding rural areas, on a regional level.

3- To map the spatial pattern of temperature for Erbil City by using the thermal band of ETM+ satellite for autumn 2011 to analyze the influence of different types of buildings and green areas on temperature patterns.

1.7 Research hypothesis

There are several factors (transport, industry, commercial and household activities) that influence the air temperature in an urban area and make it to differ from the air temperature of surrounding area (EPA, 2009a). Accordingly, the hypothesis of this study was that the air temperature (mainly minimum temperature) has increased due to the urban growth of Erbil City.

2. Study Area

The city of Erbil (36°11′28″N 44°0′33″E) is located in the northeast of Iraq and is the capital of Iraqi Kurdistan Region (Figure 6). Erbil it is one of the oldest continuously inhabited cities in the world and has an urban life that could be dated back to at least 6000 BC (UNESCO, 2010). The city has a surface area of 130 km^2. As of October 2008, the population within the Erbil urban area was 1,025,000, making it one of the largest cities in Iraq (KRG, 2012). Erbil is located in a relatively plain area and has an average elevation of 426 meters above sea level (Ayad, 2010).

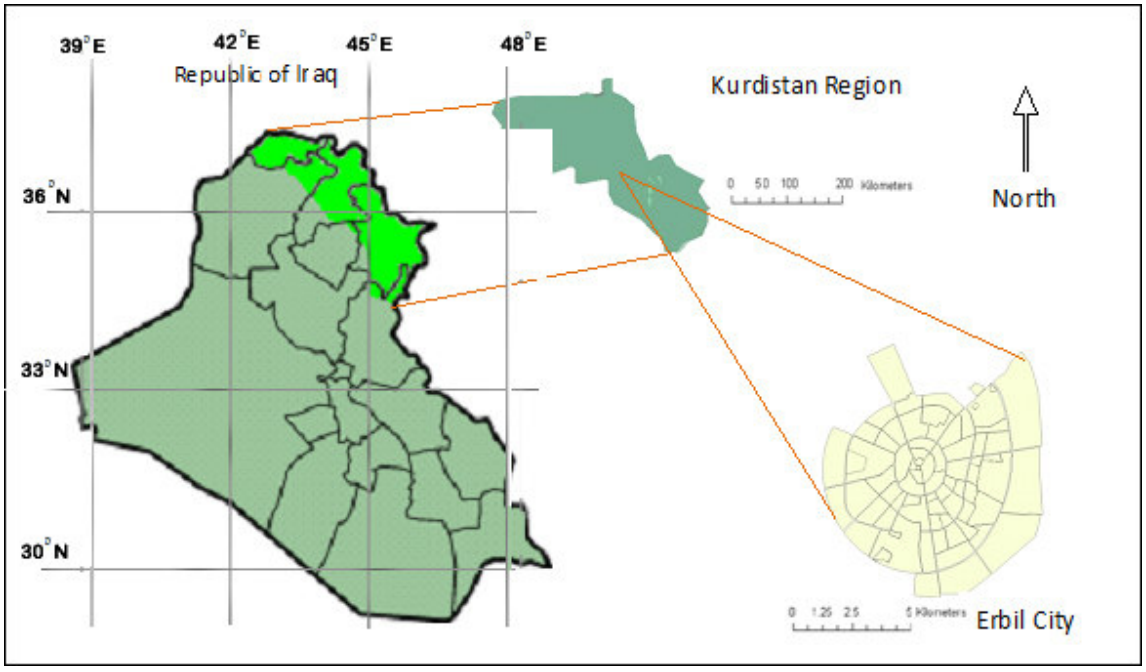

Figure 6: Map of the study area.

2.1 Climate of Erbil

Erbil City, according to Köppen's climate classification system, is located in a transitional climate zone between the Mediterranean climate (Csa) and the Arid climate (Bwh) (see Tables 1 and 2 for description of Csa and Bwh climates) (Climate, 2007). The climate is characterized by a warm to hot summer and a cold to pleasantly mild winter. However, night-

time temperatures may be low, and subzero temperatures is uncommon in the city. During the hottest part of the day during summer air temperatures may rise above 50°C. Erbil receives an average total rainfall range of 300-400 millimeters per annum, which is concentrated within the period of October to April. Summers are extremely dry; winters are fairly wet (Figure 7).The average annual relative humidity of Erbil is about 35% and the average air temperatures in Erbil for each month of the year are displayed in (Figure 8), (Ministry of Agriculture, 2012).

Table 1: Köppen's definition of Mediterranean Climate (Csa) (Climate, 2007).

Symbol	**Description**
C	Hot moderate climate. Three coldest months' average temperature between -3°C to 18°C. Warmest month average temperature > 10°C. The summer and winter seasons are well defined.
S	Dry season in summer.
A	Hot summer. Average temperature of the warmest month > 22°C.

Table 2: Köppen's definition of an arid climate (Bwh) (Climate, 2007).

Symbol	**Description**
B	Dry climate/desert. Annual evaporation higher than precipitation. No permanent rivers.
W	Dry (Arid and semi-arid) climates, Annual precipitations < 250 mm.
H	Dry and heat. Annual average temperature > 18°C.

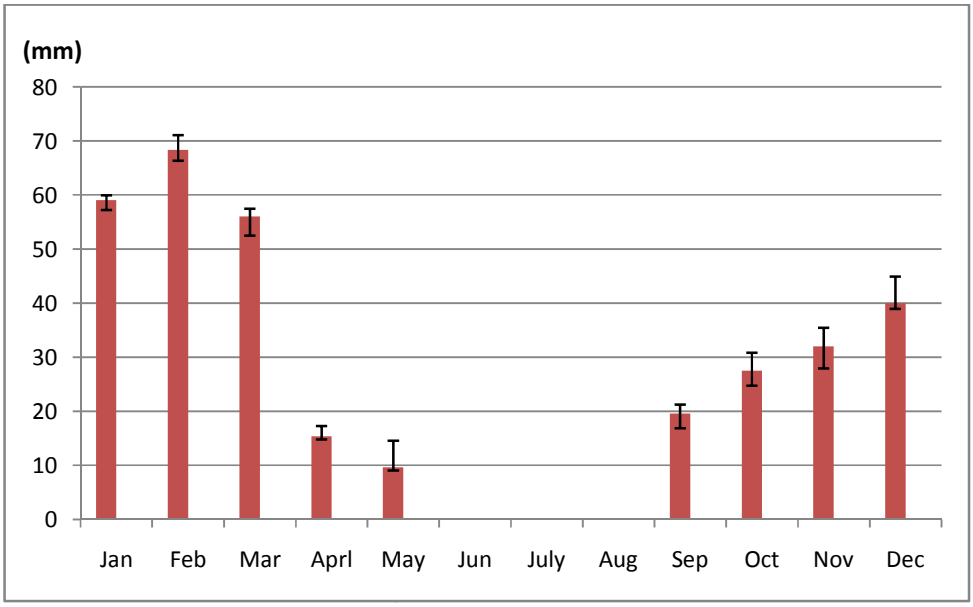

Figure 7: Erbil City mean monthly rainfall (mm) 2004-2011 (adapted from Ministry of Agriculture, 2012).

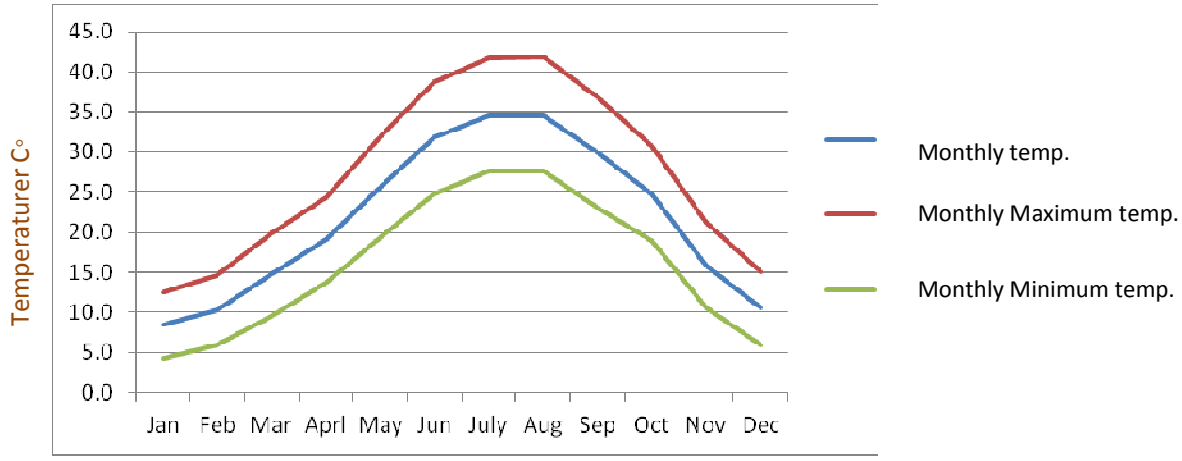

Figure 8: Monthly averages of air temperature, maximum daily temperature and minimum daily temperature in Erbil, 2000-2011 (adapted from Ministry of Agriculture, 2012).

2.2 Erbil as a Study Area

Over the past two decades Erbil has witnessed major investments in its infrastructure as well as a massive growth in its commercial activities, particularly during the second half of the last decade. Erbil is considered to be the economically strongest and most developed city in Iraq for several reasons, the most important of which is that it is the capital of the strategically important Kurdistan Region, where the Kurdish ministries, Parliament, Airport and the newly expanded infrastructure exist. Furthermore, the political and continual conflicts in the rest of Iraq have fostered the Kurdish area, particularly Erbil, to be the most secure and safe city for residency and seeking a job in Iraq. In March 2008, the International Organization for Migration (IOM, 2008) assessed that 2.7 million Iraqis had been displaced within Iraq during the preceding decade, and most of these people moved to Kurdish cities in the north. This naturally results in urban expansion.

Regardless of human immigration from the rest of Iraq to Erbil, there are a number of reasons why Erbil is an ideal area for studying the environmental influences of urbanization. Erbil City has high summer temperatures, which makes the urban area, predisposed to generate heat islands. The city is located in a plain area relatively distant from mountains and their effects, and there are no permanent rivers, lakes or any other forms of water bodies within or near the city. Regardless the global change in the climate, the city local climate has been affected by continual altering of vegetated land to more constructed areas (Salahuddin et al., 2010). The historical evolution of gardens in the city might have an influence on its local climate. The gardens in the old city, namely the citadel of Erbil and the commercial area around the citadel, representing the first and second stages of the city life (Figure 9), used to be central gardens located normally in the middle of residential areas and to have small areas. The city started to expand in the second half of the twentieth century in a modern pattern around the center in a circular direction; the third and fourth stages. These expanded areas are distinguished by frontal gardens, having a larger area than the central ones. The final stage of the city expansion is dominated by commercial aspects, such as building more high buildings and houses of smaller areas, with smaller or no gardens (Salahuddin et al., 2010). According to the new trend of expansion in Erbil City, the thermal environment of the city has been noticeably affected and this in turn could lead to discomfort and respiratory related problems. To reduce the city UHI intensity and avoiding further consequences of urban expansion, there is a need to improve the urban planning of the city. The analysis presented in the following chapters

provides an explanation of the UHI in Erbil that might be used as a basis for decision making regarding urban and ecological planning in Erbil City.

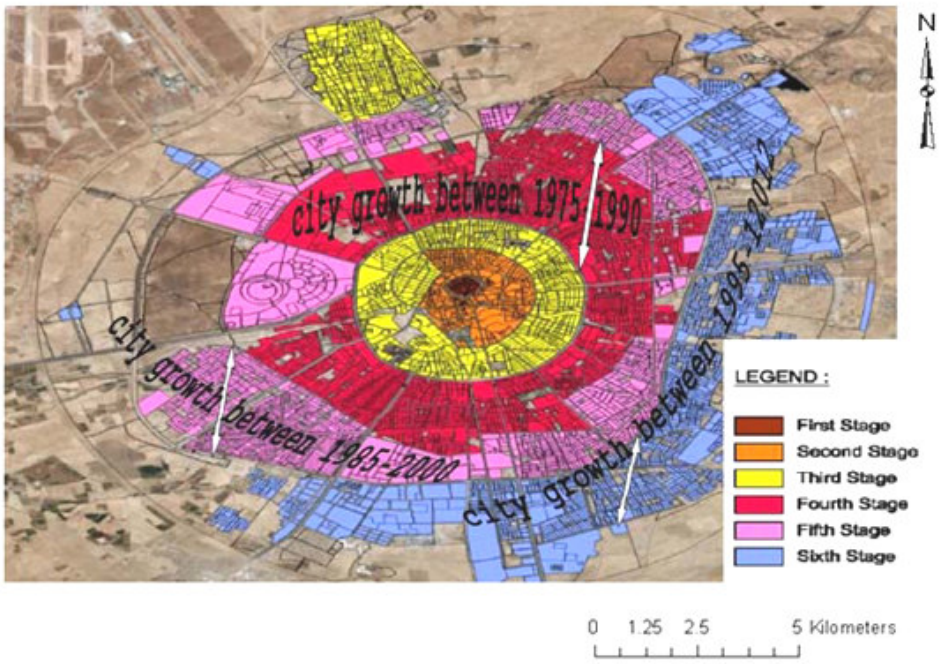

Figure 9: The historical development of Erbil City (Erbil City Master Plan Report, 2007).

3. Data and Methodology

3.1 Meteorological Data

In order to analyze the effect of urbanization on the local climate of Erbil City and its surroundings, there was a need to make two databases.

3.1.1 Temporal Data

Daily records of air temperatures from eight weather stations (Figure 10) were obtained from the Ministry of Agriculture in Erbil, which includes the maximum and minimum temperatures registered daily at the weather stations, then grouped in monthly and annual averages, except for the urban station of Erbil (1975 to 2011) all the other station have a time series of 1985-2011 (Table 3). In accordance to this information, and to identify the variability of the temperature in the time series, the following statistical tests were applied.

First of all, to reject the null hypothesis, which claims that the sample data come from a population with a normal distribution and are not influenced by some non-random causes, there is a need to calculate skewness (z1), kurtosis (z2) and standardized coefficients (Siegel, 1956). In case of the absolute value of z2 or z1 being more than 1.96, then a significant deviation of the curve is indicated at the reliability level of 0.95.

For evaluating the air temperature trend, a simple regression analysis was performed with the year as independent variable and the temperature as dependent variable, with determining the significance for type I error of 5% ($\alpha = 0.05$) and the coefficient of determination R2 was 0.74. The analysis was applied for the whole period of 1975-2012 for Erbil urban station, the only time series available in the ministry of agriculture.

In order to reinforce the validity of the simple regression analysis there is a need to apply the Kendall-t rank correlation as a non-parametric alternative. Balling and Ceverny (1987) stated that to identify any temporal linear or non-linear trend in the annual data from all the stations, it is necessary to apply the Mann-Kendall rank statistic. Moreover, between Erbil station and each one of the other stations, the monthly and annual air temperature differences were calculated for both minimum and maximum values. The data from the rural stations were available only from 1984 onwards. All the means, correlation coefficients and standard deviations between the year of record and the temperature differences were all calculated.

The time series was divided into three shorter periods of 1975-1990, 1985-2000 and 1995-2011, the statistical reason for using overlapping data is the case of missing observations and extreme values at the end of the time series (Edgerton, 1996). The three time sections was selected to reflect the growth of the city, whereby each period represents a social, political or commercial change that the city has experienced (Figure 9).

In order to determine if the annual and monthly air temperatures in the three sub-periods have any significant changes through time, the student t test was used (Arnfield, 2003). The statistical test has a value of 1.95, reflecting a double-tailed test with 95% reliability.

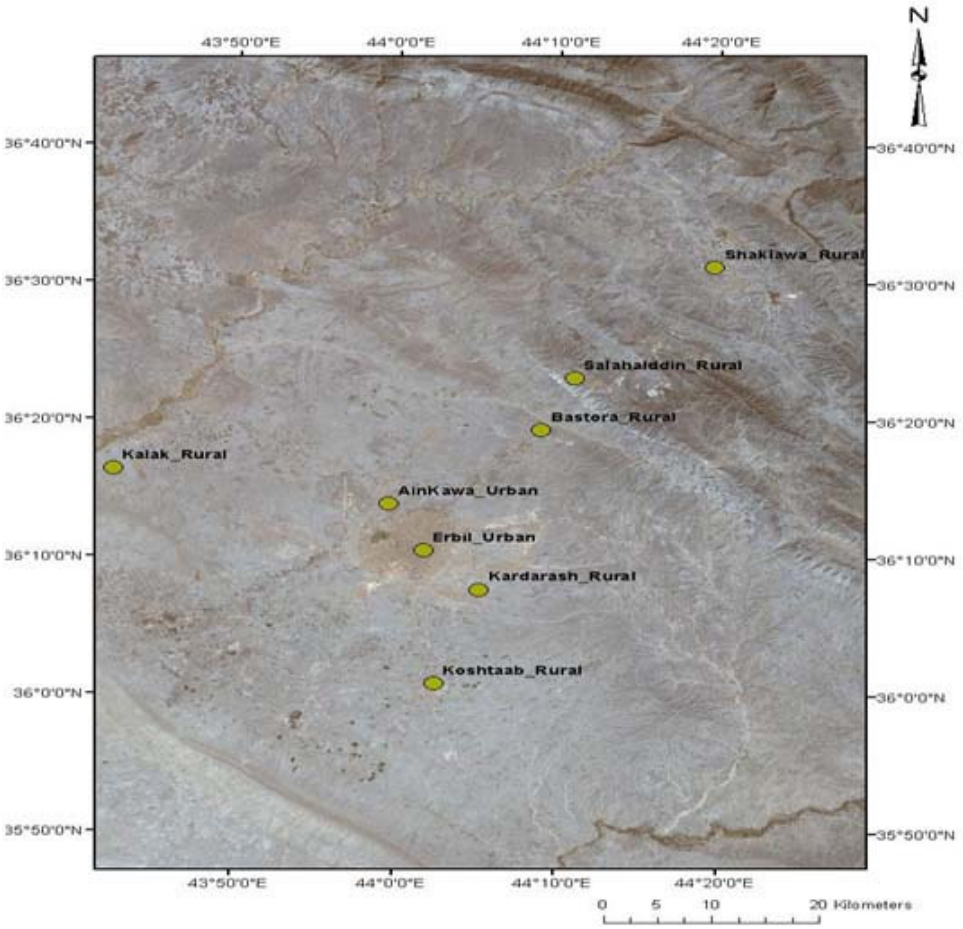

Figure 4: All weather stations location that used in spatial and temporal analyses.

3.1.2 Spatial Data

Around Erbil City there is a possibility to find more weather station data (Table 3 and Figure 11).Except for Erbil station that consider to be an urban , all the other station are rural.

Ainkawa station is the nearest one to Erbil where is far about 10 Km. Kardarash, Khoshtaab and Bastora stations are located in small villages around Erbil City. Shaklawa and Salahalddin stations are located in high elevated area where Kalak have the lowest elevation and surrounded by a small forest. Almost, all these stations are not suitable to be involved in a long time series analysis due to their short time record of temperature. However, these weather stations could be used to perform spatial analysis of temperature. A time series of 2004-2011 was used in the analysis, which includes generating seasonal averages of the maximum and minimum temperatures. This seasonal variability was produced spatial coverage for four seasons using Inverse Distance Weight (IDW) interpolation. The IDW interpolation was used because it was easy to apply with no special requirements and it was fast and has a certainty for interpolation (H. X. Chai et al, 2011). The seasons are autumn/fall comprises September, October and November; winter is December, January and February; spring is March, April and May; and summer is June, July and August.

Table 3: weather stations used in the temporal and spatial analysis.

Weather station	Time series	Latitude (°N) (Decimal Degrees)	Longitude (°E) (Decimal Degrees)	Altitude (masl)
Erbil (Urban)	1975-2011	36° 125	44° 025	420
Ainkawa	1985-2011	36° 14	44° 015	434
Kardarash	1985-2011	36° 07	44° 01	410
Kalak	1985-2011	36° 17	43° 44	252
Khoshtaab	1985-2011	35° 46	43° 35	275
Bastora	1985-2011	36°20	44° 10	270
Shaklawa	1985-2011	36° 25	43° 15	950
Salahalddin	1985-2011	36° 24	44° 014	1050

3.2 Satellite Data

To derive LST and NDVI over the study area a Landsat 7 ETM+ image acquired on September 14th 2011 was used. The image was captured at approximately 2:55 pm local time under clear atmospheric conditions (0% cloud coverage). The image was obtained from the United States Geological Survey (USGS).At the day of image capture the air temperature in Erbil was approximately 34°C and the humidity was 15% (Ministry of Agriculture, 2012).

3.2.1 LULC Data

The shape file with LULC data for Erbil City was acquired from Erbil Municipality. It was produced in 2011 with a base map scale of 1:12500, including details about all LULC in the city. These LULC represent neighborhoods, main roads, streets, bare land and parks. In later sections there will be more detail on reclassifying the main shape file according to vegetation distribution and kinds of built up area inside Erbil City.

3.2.2 Satellite Imagery Pre-processing

Because of Landsat 7 ETM+ image was captured under clear conditions (0% cloud coverage), no atmospheric corrections were applied and uniform atmospheric conditions in the image are assumed. The USGS has preprocessed the image in order to rectify any radiometric or geometric distortions of the image in order to acquire the level 1G product. Usually the correction process involves both ground control points and digital elevation models to have a product that is free from any sort of distortions could be associated with the satellite (deviations of attitude from the nominal), sensor (effects of view angel) and Earth (rotation, curvature). The image also was geometrically corrected and geo-referenced by the USGS to Universal Transverse Mercator (UTM) zone 29N coordinate system and the WGS1984 datum (USGS, 2010b; Landsat Project Science Office, 2001).

3.2.3 LULC Data Preparation

As mentioned above, the shape file was acquired from Erbil Municipality depicting LULC for Erbil City, and it was rectified by the municipality to the WGS1984 datum and UTM zone 29N coordinate system. The shape file represents the study area which includes only the urban core of Erbil City where the UHIs are more likely to develop. This shape file was used to indicate which types of urban LULC are determining the urban thermal environment.

The presence and the percentage of vegetation in the city have a vital role in this study. Accordingly, the LULC shape file was reclassified to the classes Vegetated area (park), Houses with gardens, Houses with no gardens, Area with sparse vegetation (commercial) and Area with no vegetation (industrial),(Table 4 and Figure11). The emissivity values in turn were derived for each class see 3.2.4 section, to be involved later in the calculation of the land surface temperature.

Table 4: new classes used in the study.

The new classes	Reclassified classes
Green area	Purely vegetated areas and parks.
Houses with frontal gardens	The area indicated as the third stage of the city life (Figure 10), where almost all the modern houses exist.
Commercial and houses with central gardens	The area indicated as the first and second stages(Figure 10), where there are small gardens and retail shops.
Mixed houses with bare soil	Area consists of newly built houses bordered with bare soil located in the eastern part of the city.
Industrial area	The area fully consists of car services without any sort of vegetation.
No gardens houses	Area located to the west of the city consists of small sizes houses and almost No gardens.

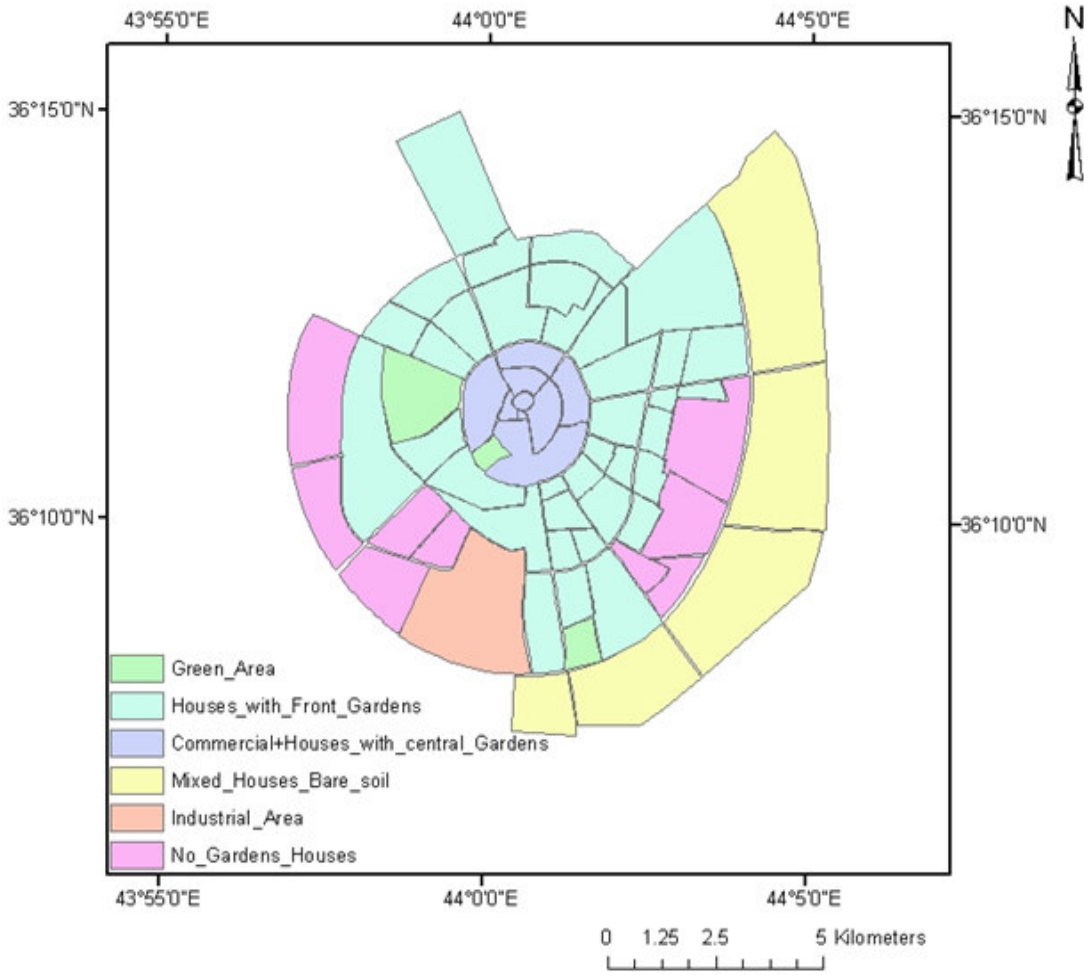

Figure 5: Spatial patterns of LULC within the study area.

3.2.4 Data Processing

Calculation of NDVI

Band 4 the near-infrared a part of the electromagnetic spectrum (0.75-0.90 μm) and band 3 the red (0.63-0.69 μm) of the Landsat 7 ETM+ image acquired on September 14th2011 were used to calculate NDVI for the study area (NASA, 2010), using the equations explained below.

Conversion of the Digital Number to Spectral Radiance

To calculate NDVI from Landsat ETM+ data there is a need to convert the digital numbers (DN) of bands 4 and 3 to spectral radiance by using Equation (1) (Landsat Project Science Office, 2001):

$$L_\lambda = ((LMAX_\lambda - LMIN_\lambda)/ (QCALMAX-QCALMIN)) * (QCAL-QCALMIN) + LMIN_\lambda \quad (1)$$

Where $LMIN_\lambda$ is the spectral radiance scaled to QCALMIN (-5.1 Wm-2sr-1μm-1 for band 4 and -5.0 Wm-2sr-1μm-1 for band 3); LMAXλ is the spectral radiance scaled to QCALMAX (241.1 Wm-2sr-1μm-1 for band 4 and 234.4 Wm-2sr-1μm-1 for band 3); QCAL is the DN; QCALMAX is the maximum quantized calibrated value of the pixel in DN (255) ; QCALMIN is the minimum quantized calibrated value of the pixel in DN (0); and Lλ is the spectral radiance at the sensor's aperture in $Wm^{-2}sr^{-1}$-1μm-1.

The Landsat Project Science Office (2001) was the provider of the values in Equation (1), with referencing to metadata which accompanied the ETM+ image.

Conversion of Spectral Radiance to Planetary Reflectance

The Spectral radiance for band 4 and 3 were transformed to planetary reflectance (Landsat Project Science Office, 2001):

$$\rho_p = \pi L_\lambda d^2/ (ESUN_\lambda \cos\theta) \quad (2)$$

Where: L_λ is the spectral radiance at the sensor's aperture in $Wm^{-2}sr^{-1}\mu m^{-1}$; d is the Earth–Sun distance in astronomical units (1.01142863021849); $ESUN_\lambda$ is the mean solar exo-atmospheric irradiance (1039 for band 4 and 1533 for band 3); θ is the solar zenith angle in

degrees and ρ_p is the planetary reflectance. All the values were obtained from (Landsat Project Science Office, 2001).

Calculation of NDVI

According to Tam et al (2010) methodology, the NDVI was calculated by using the reflectance values from the near-infrared (ρ_{nir}) and red (ρ_{red}) channels.

$$NDVI = (\rho_{nir} - \rho_{red})/ (\rho_{nir} + \rho_{red}) \quad (3)$$

Derivation of LST

The thermal band (10.4-12.5 μm) of the September 14th2011 Landsat 7 ETM+ sensor with 30 m resolution was used to extract the LSTs over the study area (NASA, 2010).

Conversion of the Digital Number to Spectral Radiance

By using Equation (1), the DNs of thermal band from the Landsat 7 ETM+ image captured on September 14th 2011 were firstly converted to spectral radiance.

Conversion of Spectral Radiance to Radiant Surface Temperature

Equation (4) is used to convert spectral radiance values for thermal band to radiant surface temperature. It should be noted that the conversion should be carried out with the assumption of uniform emissivity, by using the pre-launch calibration constants for the Landsat ETM+ sensor (Landsat Project Science Office, 2001). Uniform emissivity means that all the calculated radiant surface temperatures are referenced to a blackbody. A simple definition for the blackbody is any surface that absorbs all incident electromagnetic radiant energy and neither transmits nor reflects this energy, for that a blackbody can be an ideal radiator (Artis and Carnahan, 1982).

$$TB= K2/ (\ln(K1/ L\lambda + 1)) \quad (4)$$

K1: calibration constant 1 (666.09 $Wm^{-2}sr^{-1}\mu m^{-1}$)

K2: calibration constant 2 (1282.71 K)

L_λ: the spectral radiance at sensor in $Wm^{-2}sr^{-1}\mu m^{-1}$

T_B: radiant surface temperature (in Kelvin) brightness temperature at satellite

Landsat Project Science Office (2001) is the provider of calibration constants values used in Equation (4).

Estimation of Emissivity

Emissivity is a ratio between the spectral radiant emittance of a surface to that of a blackbody at a similar temperature (Artis and Carnahan, 1982). However, the radiant surfaces temperatures derived from Equation (4) are referenced to a blackbody; it is necessary to make a correction for land surface emissivity according to the nature of each object surfaces. The emissivity of a surface has values between 0 and 1. Most natural objects could have a spectral emissivity is close to 1. The land surface emissivity value of any LULC is influenced by the effect of several factors such as: roughness, moisture content and chemical composition (Stathopoulou et al., 2007).

According to the methodology of Stathopoulou et al. (2007), one must make a correction for mean surface emissivity of each LULC. The method tries to obtain surface emissivity values from the NDVI already calculated in Equations (1-3), taking into consideration the three different cases outlined below:

A. NDVI > 0.5

Any pixel with NDVI higher than 0.5 is assumed to be fully vegetated (well treed park) and all these pixels are having an assumed emissivity value of 0.98 (Schmugge and Coll, 1998) .

B. NDVI < 0.2

NDVI lower than 0.2 are assumed to be man-made materials or mixed pixels between man-made materials and sparse vegetation. The emissivity (ε) values are typically calculated from the reflectivity values (ρ) in the red channel, Equation (5).

$$\varepsilon = 1 - \rho_{red} \qquad (5)$$

C. $0.2 \leq NDVI \leq 0.5$

In case of pixels that are a mixture of man-made materials and vegetation these pixels are assigned an NDVI values less than or equal to 0.5 or greater than or equal to 0.2. For emissivity calculation of this case, there is a need to use Equation (6):

$$\varepsilon = \varepsilon v Pv + \varepsilon m(1 - Pv) + d\varepsilon \quad (6)$$

$d\varepsilon$:the fraction of emissivity caused by internal reflections/cavity effect (Equation 8)

P_v: the vegetation proportion (see Equation 7, below)

ε_m: the emissivity of man-made materials (0.92)

ε_v: the emissivity of vegetation (0.98)

ε : emissivity.

$$P_v = (NDVI - NDVI_{min})^2 / (NDVI_{max} - NDVI_{min})^2 \quad (7)$$

Where: $NDVI_{min}$ is 0.2, and $NDVI_{max}$ is 0.5.

Equation (8) is used to find out the $d\varepsilon$ value:

$$d\varepsilon = (1 - \varepsilon_m)\varepsilon_v F(1 - P_v) \quad (8)$$

F: is the shape factor regarding the vegetation geometrical structure, whose mean value is 0.55, in case of considering different geometrical distributions (Sobrino et al., 1990).

Then mean emissivity values were finally computed for each LULC type by using the Zonal Statistics function in ESRI's ArcGIS™ software (Table 5).

Table 5: Surface emissivity values of each LULC type.

LULC type	**Emissivity**
Green area (park)	0.959637
Houses with frontal gardens	0.931769
Mixed commercial and houses with central gardens	0.929153
Mixed houses and bare soil	0.927825
Almost houses without gardens	0.918918
Industrial area	0.894443

Extracting LST from Radiant Surface Temperatures

The final step is correcting the radiant surface temperatures by using emissivity values from Table 3 to obtain the LST by the Equation (9):

$$LST = T_B / (1 + (\lambda T_B / \rho) \ln\varepsilon \quad (9)$$

Where ε: emissivity; $\rho = h \times c/\sigma$ (1.438×10^{-2} m K), h : Planck's constant (6.26×10^{-34}J s), c : the velocity of light (2.998×10^{8} m/sec); σ: Ludwig Boltzmann's constant (1.38×10^{-23}J K^{-1}), λ : the wavelength of emitted radiance (11.5 μm), T_B : radiant surface temperature (Kelvin); and LST: land surface temperature (Kelvin). The value of Kelvin converted to Celsius by subtracting it from 273.15 (Artis and Carnahan, 1982). Finally, mean computation of NDVI and LST by the type of LULC were derived by means of a zonal summary GIS operation.

4. Results

This chapter reviews the main results and their analyses. All the results are related to the effect of urbanization on local climate of Erbil City. The results were divided according to their source of data as presented below.

4.1 Ground Weather Stations

This section presents the results related to the ground weather stations, which in turn have been divided into two subsections according to the temporal and spatial analysis of the data.

4.1.1 Temporal Analyses

To observe the impact of urban expansion on the local climate of any city, Landsberg (1975) suggested that the monthly minimum temperatures should be used since they are more affected by urban growth than maximum ones. The average minimum temperatures for Erbil urban weather station during the month of January, February, December and July and its tendency for the 1975-2011 period, is shown in Figure 12,13 ,14 and 15 respectively. January, February and December were selected because they considered being the coldest month Erbil City experiences during the year. The July month was also plotted to represents the warmest month. Furthermore, basic statistics with a similar tendency were estimated for all the months together in Table 6.

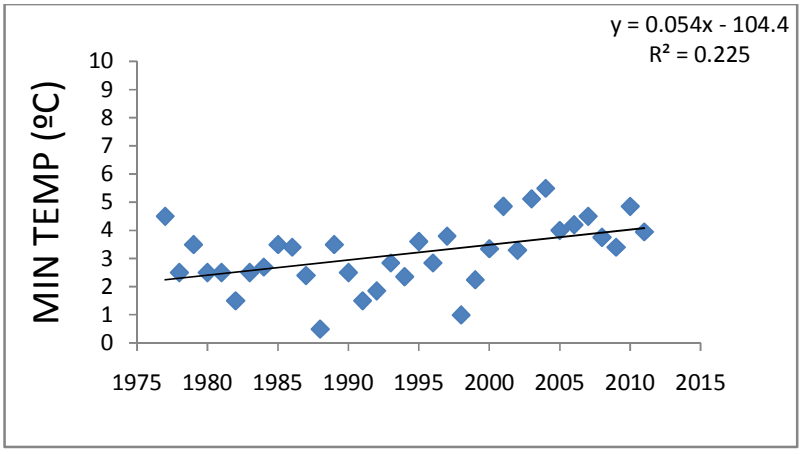

Figure 12: Minimum temperature trend in urban Erbil in January, 1975-2011.

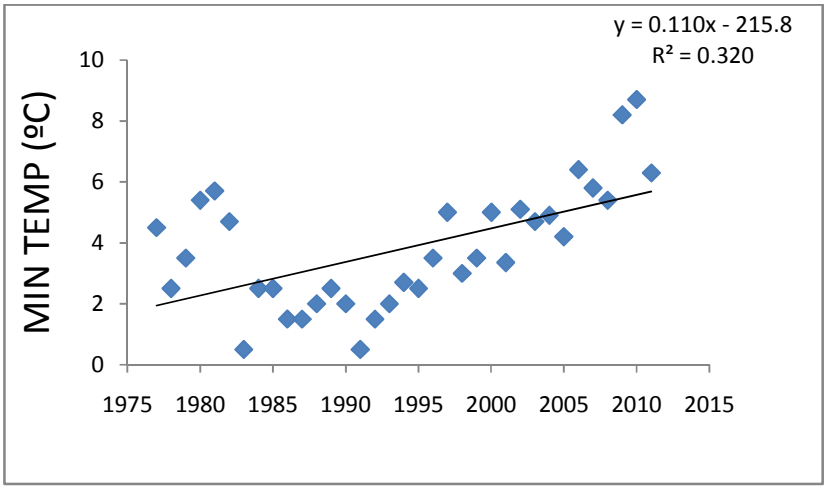

Figure 6: Minimum temperature trend in urban Erbil in February, 1975-2011.

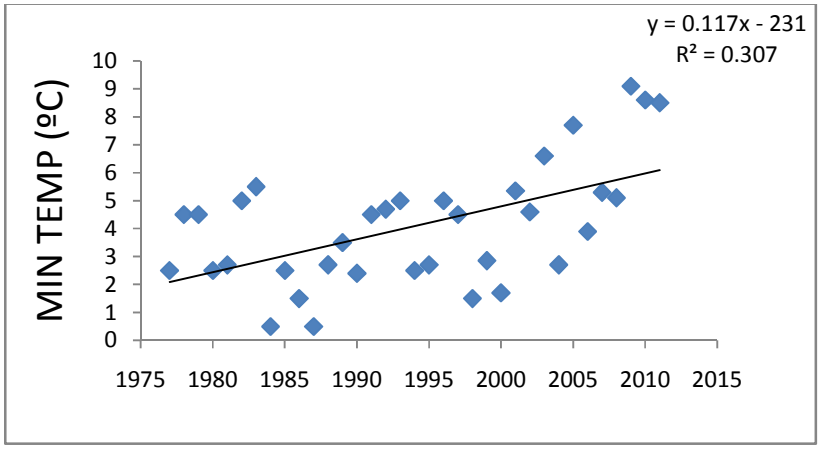

Figure 7: Minimum temperature trend in urban Erbil in December, 1975-2011.

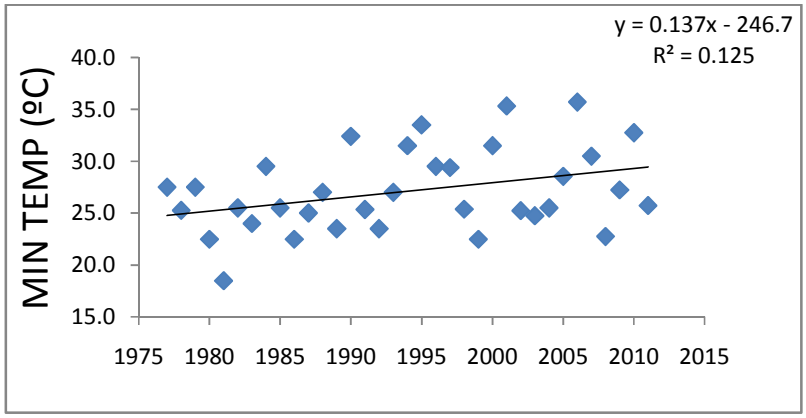

Figure 8: Minimum temperature trend in urban Erbil in July, 1975-2011.

Table 6: descriptive statistics of the time series of mean minimum air temperature ($T_{a,min}$) at Erbil urban (1975-2011), where std is the standard deviation, z_1 is the skewness, z_2 is the kurtosis, $R_2$is the regression determination coefficient, K.T is a Kendall-t non-parametric correlation coefficient, and b is the slope of the regression line.

Month	$T_{a, min(°C)}$	std	Z_1	Z_2	R_2	K.T	b
Jan	2.7	1.9	0.87	1.89	0.22	0.32	0.075
Feb	3.4	2.1	0.85	0.33	0.32	0.45	0.085
March	6.3	2.8	0.48	-0.39	0.37	0.12	0.056
April	11.1	3.3	-0.54	-0.16	0.15	0.05	0.023
May	17.2	2.5	-0.22	-0.53	0.18	0.21	0.038
June	22.9	2.0	0.05	-0.60	0.29	0.37	0.059
July	25.9	1.7	-0.48	0.53	0.12	0.3	0.041
Aug	26.0	1.9	0.17	-0.07	0.21	0.45	0.057
Sep	21.9	1.6	0.23	0.01	0.31	0.39	0.05
Oct	19.2	1.4	-0.60	-0.25	0.25	0.55	0.027
Nov	11.6	1.3	-0.46	-1.24	0.15	0.57	0.073
Dec	3.4	2.4	0.91	0.30	0.30	0.35	0.084
Annual	14.3						0.055

In Table 6, both the skewness and kurtosis indicate that there is no significant deviation from normal for any month, which precludes the application of any transformation method to the data. It can be observed that the monthly series in the table presents components of random variance. In accordance to the value of determination coefficient, and the Kendall-t non-parametric correlation coefficient, most of the correlations found tend to be significant, with a 95% reliability level. The b parameter in Table 6 explains the thermometric trend, which indicates a trend toward temperature increase at a rate of 0.055°C/year warming annually (1.95°C in 35 years), while December (0.084°C/year) and February (0.085°C/year) show the greatest warming at a monthly level.

All the statistics tests have been applied on the maximum temperature as well; the behavior of the data was indicating a kind of normality and randomness. However, the analyses show a negative trend in some months. For example, the month of November showed the highest value of negative trend (–0.052°C/year), and for the positive trend the month of May and June they showed a value of 0.045 and 0.047 °C/year respectively. Accordingly, the less increasing in the maximum temperature compare to the minimum temperature and the contradicting in the results some months obtained from the analyses of maximum temperature (appendix I),

made it evident that the most important temperature modification has been indicated in the minimum values. The obtained results might indicate a significant increase in the minimum temperature; however this is compatible with most studies (Landsberg, 1975).

In order to analyze the temperature variation in more details over the whole period of the study area, there was a need to divide the time series in to three sub-series, as described previously (1975-1990, period I; 1985-2000, period II; 1995-2011, period III). The differences in the minimum temperatures for the 1975-1990 and 1985-2000 periods are not significant at a 95% reliability level (Table 7). However, there is some statistical significance when comparing the difference in the means among the 1975-1990 and 1995-2012 (I –III), and the 1985-2000 and 1995-2012 (II –III) periods. The difference in the means among the three periods is probably related to the changes in the land use and fast city growth around the urban weather station in the third period of the city life.

Table 7: Mean minimum temperature in urban Erbil 1975-1990 (I), 1985-2000 (II), 1995-2012 (III) periods and student t test application to show the significance in the difference of the means.

	I 1975 1992	II 1985 2000	III 1995 2011	Student's t I-II	Student's t II-III	Student's t I-III
Jan	2.85	3.25	4.1	1.25	3.75	3.97
Feb	3.50	4.25	5.3	1.55	3.85	4.95
Mar	6.85	7.25	8.7	0.84	2.85	3.95
Apr	12.27	12.75	13.4	0.65	1.75	2.17
May	17.95	18.25	19.3	0.75	1.85	2.84
Jun	23.25	23.55	24.6	0.94	3.22	4.75
Jul	25.31	25.60	26.8	1	2.25	3.21
Aug	26.45	26.25	27.3	-0.17	2.55	2.25
Sep	21.85	22.25	23.0	0.95	2.54	3.27
Oct	18.75	18.95	19.4	0.85	3.95	4.87
Nov	9.85	10.25	11.2	0.1	2.44	3.74
Dec	3.25	4.25	5.4	2.25	2.95	4.55
Annual	14.34	14.74	15.70	2.44	3.25	7.75

Statistically significant values at the 95% reliability value.

It can be seen from Table 7 that there are a statistically significant values at 95% reliability value when applying the student's t test between the period III and the other two periods. According to the obtained results, it can be noticed that the minimum temperature has been ascending over the past decade in Erbil urban area.

To understand the trend of minimum temperature over the time in Erbil City and compare it to the trend of surroundings rural stations, the linear trends were obtained for Erbil urban and for three rural stations (Table 8). To quantify the intensity of the UHI the differences in the urban-rural minimum temperature were calculated from these trends (Table 9).

The thermal differences in urban-rural minimum temperature reflect the degree of the intensity for the UHI phenomenon (Jáuregui, 1997). According to the results shown in Table 8, there is an indicator for significant and positive trends of the minimum temperatures, with a higher trend of warming for Erbil Urban. Furthermore, the statistically significant and positive trends that document the warming of Erbil weather station comparing to the rural stations could be noticed in Table 9. The greatest annual trend in thermal differences was between Erbil and Kalak with 0.055°C/year, and followed by the urban station of Erbil and Kardarash the rural station, with 0.051°C/year. However, the differences between Erbil urban and Ainkawa record a less significant value compare to the other two rural stations. To have a slight difference between Ainkawa station and Erbil urban station could be a good indicator of the effect of urbanization on the modifying of minimum temperatures; in other words, Ainkawa area is considered to be very attached to Erbil City and witnessed as well urban growth in last decade.

Table 8: Linear trends of minimum temperature of Erbil urban and other rural stations

Weather Station	Distance in (Km)	Period	Jan	Feb	Mar	Apr	May	Jun	July	Aug	Sep	Oct	Nov	Dec	Annual	R2 for Annual
Erbil	0	1985-2011	0.077	0.085	0.054	0.027	0.039	0.058	0.044	0.047	0.057	0.05	0.074	0.087	0.074	0.518
Ainkawa	10	1985-2011	0.072	0.072	0.050	0.025	0.035	0.055	0.032	0.045	0.04	0.047	0.052	0.045	0.057	0.535
Kardarash	8.5	1985-2011	0.047	0.050	0.052	0.0047	0.037	0.035	0.005	0.0023	0.002	0.047	0.057	0.035	0.034	0.521
Kalak	34	1985-2011	0.045	0.048	0.015	0.0037	0.015	0.004	0.027	0.005	0.047	0.002	0.015	0.034	0.030	0.420

d: refers to the distance between Erbil urban weather station and all the other rural weather stations.

Table 9, Trends of differences in daily minimum air temperature between Erbil urban and those selected in the rural between 1985 and 2011 as a linear trends, see appendix 3 for plotting of the values as a graph.

Weather Station	Jan	Feb	Mar	Apr	May	Jun	July	Aug	Sep	Oct	Nov	Dec	Annual
Erbil - Ainkawa	0.005	0.013	0.004	0.002	0.003	0.003	0.012	0.002	0.017	0.004	0.022	0.022	0.027
Erbil - Kardarash	0.030	0.035	0.002	0.022	0.001	0.023	0.05	0.024	0.05	0.003	0.017	0.052	0.040
Erbil - Kalak	0.032	0.037	0.039	0.032	0.024	0.054	0.017	0.042	0.010	0.048	0.055	0.013	0.045

The underlined values are considered to be a significant with a type I error of 0.05 (a = 0.05).

The trend of the annual differences was also explained between Erbil station and the other rural stations (Ainkawa, Kardarash and Kalak) for the period 1985-2011, Figure (16, 17 and 18):

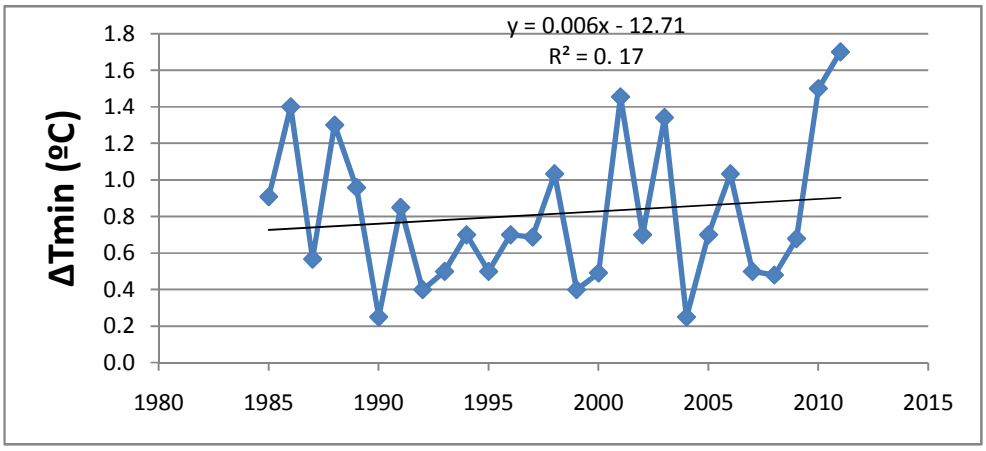

Figure 16, annual minimum temperature differences between Erbil and Ainkawa station for the period 1985-2011.

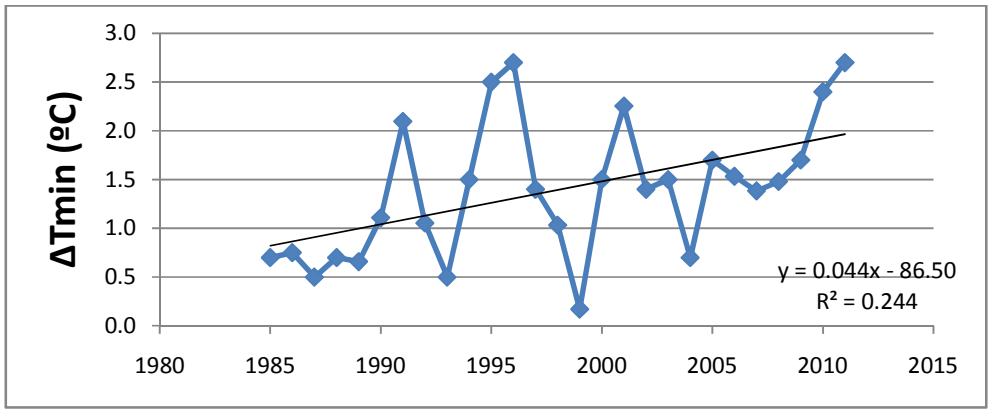

Figure 17, annual minimum temperature differences between Erbil and Kardarash station for the period 1985-2011.

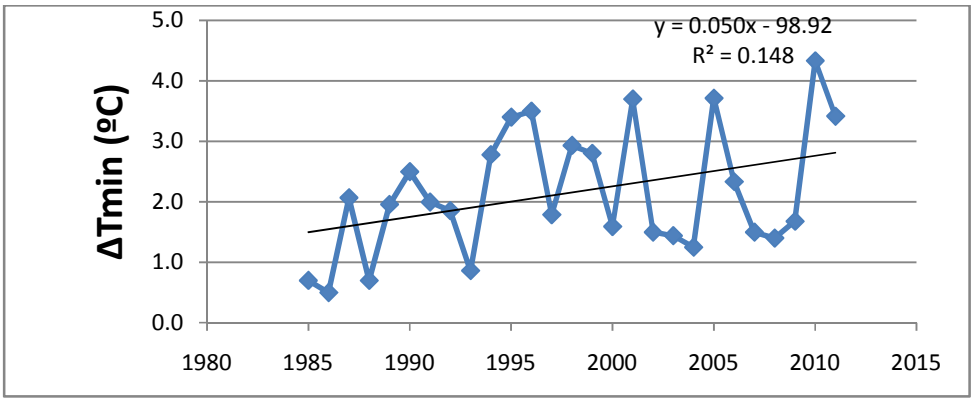

Figure 18 , annual minimum temperature differences between Erbil and Kalak station for the period 1985-2011.

It was obvious from the annual differences of minimum temperature that Erbil and Ainkawa stations have relatively slight values compare to the differences between Erbil and the other two rural stations (Kardarash and Kalak), where its likely reflect the effect of urban growth on the variation of minimum temperature among all stations.

4.1.2 Spatial Analyses

Seasonal minimum and maximum temperatures between the years 2004 and 2011are presented in Tables 10 and 11 (respectively).

Table 10: Seasonal averages of minimum temperature (°C)2004-2011.

Weather station	Station number	Autumn	Winter	Summer	Spring
Erbil Urban	1	17	4.9	26.1	13.5
Ainkawa	2	16	3.1	24.1	11.3
Kalak	3	12.3	3.25	19.7	8.2
Bastora	4	16.2	3.8	25.2	12.3
Khoshtaab	5	14.9	4.25	23.15	11.25
Salahalddin	6	15.2	3	24	11.6
Shaklawa	7	11.2	1.7	24.1	9.9

Table 11: Seasonal averages of maximum temperature (°C)2004-2011.

Weather station	Station number	Winter	Spring	Summer	Autumn
Erbil Urban	1	29.5	13.7	41.2	25.5
Ainkawa	2	29.2	13	41.5	25
Kalak	3	31.1	15.3	42.1	27
Bastora	4	29.6	14.4	41.1	25.5
Khoshtaab	5	29.3	12.9	39.5	24.7
Salahalddin	6	24.9	9.9	34.9	20
Shaklawa	7	23.5	10	36.6	20.8

After calculating the seasonal minimum and maximum temperatures for the years 2004 to 2011, the IDW interpolation was applied to plot the spatial distribution of values. It can be observed that the highest values are located in the urban zone, where the UHI is normally located. The seasonal minimum temperature distributions in winter, spring, summer and autumn are shown in Figure 19. The seasonal variation of maximum temperature are presented in Figure 20, which illustrates the similar trend as the minimum temperature when spatially distributed, but which varies less between the urban area and the surroundings. In the

northern part of the regional area low temperature values can be seen from Figure 19 and Figure 20, which are correlated with the topography of that area (mountainous terrain). Likewise, the western part of the regional area, particularly Kalak weather station, shows relatively low values of minimum temperature. This is attributable to the area having small, spatially distributed forest around the weather station. There is an obvious trend towards a warmer urban climate, which was evident from the results of the interpolation for both maximum and minimum temperatures (Figures 19 and 20). The higher values of minimum temperature for winter and autumn are obviously observed in Erbil urban weather station, which illustrates the development of the UHI, followed by spring and summer. The same trend could be observed from the nearest station, Ainkawa neighborhood. However, there might be some anomalies of these isotherms, such as Bastora that illustrating a warmer zone in winter for Figure 20 and spring and summer for Figure 21 comparing to other rural areas. This anomaly in the interpolated values might be due to the low altitude that the weather station locates Table 3.

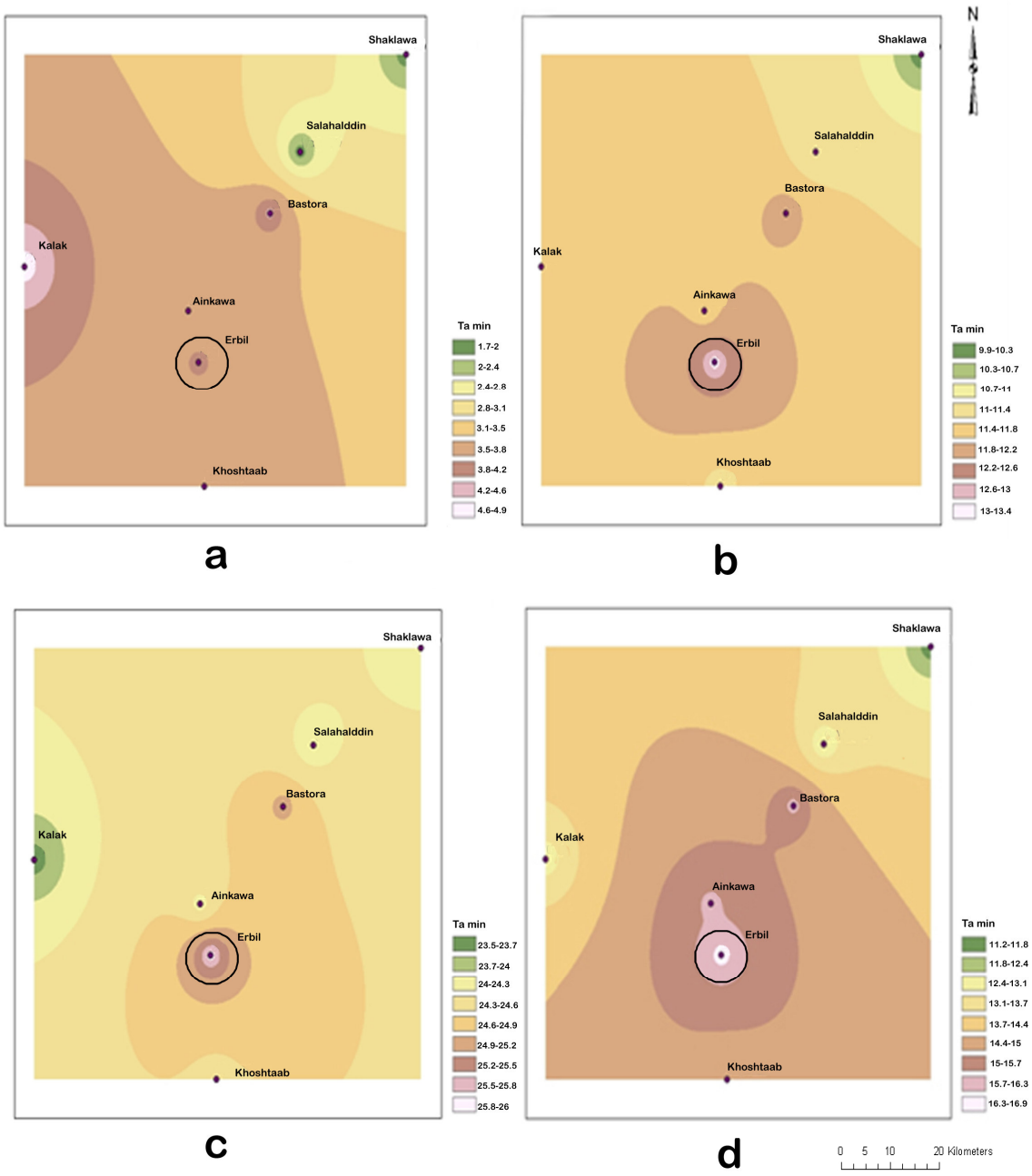

Figure 19: Minimum temperature (°C) in urban Erbil and its surrounding rural station 2004-2011 in a) winter, b) spring, c) summer and d) autumn, where Erbil Urban locate inside the virtual circle.

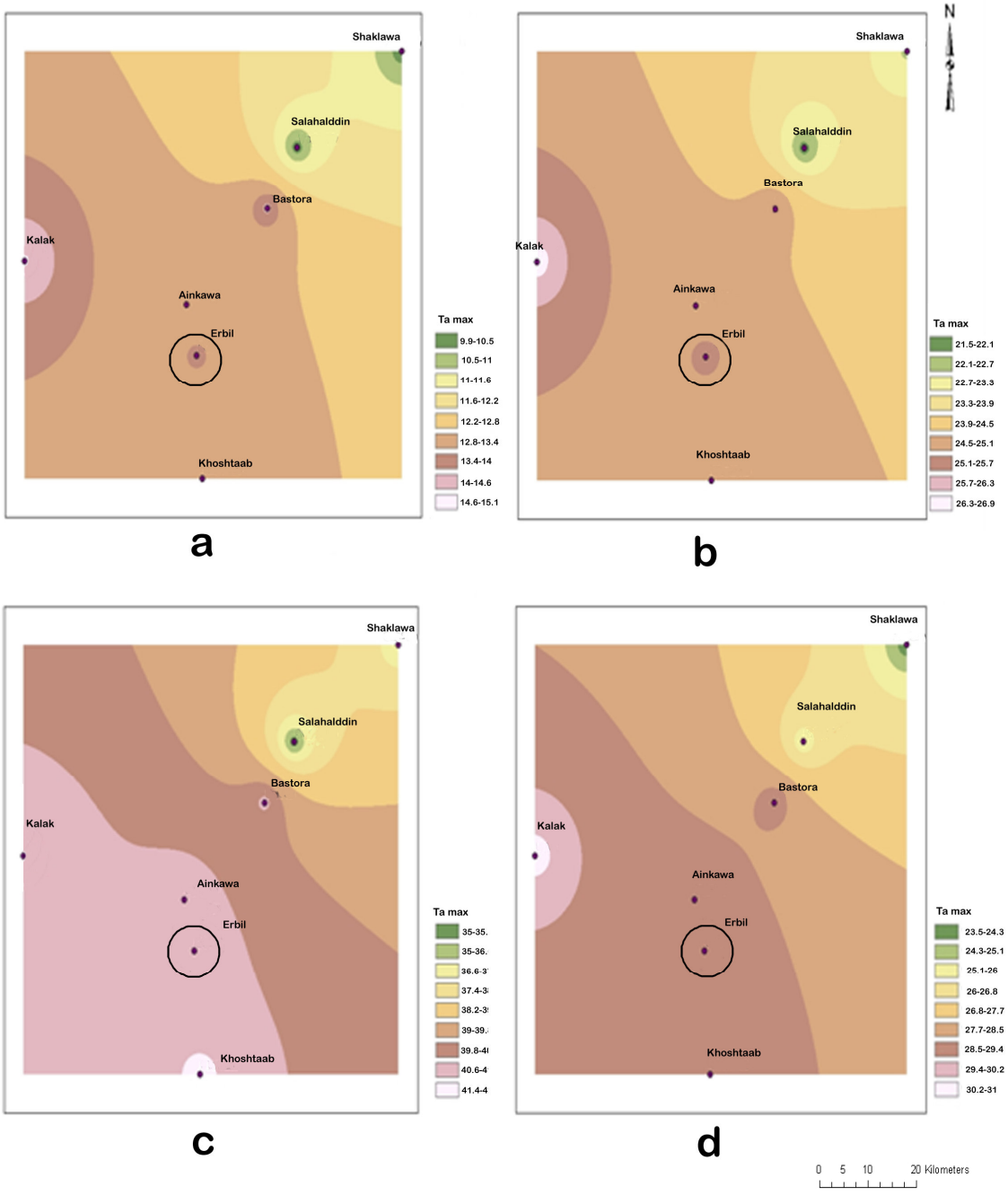

Figure 20: Maximum temperature (°C) in urban Erbil and its surrounding rural station 2004-2011 in a) winter, b) spring, c) summer and d) autumn, where Erbil Urban locate inside the virtual circle.

4.2Satellite Image Results

4.2.1 LST and NDVI Imagery Interpretation

In general there is a negative correlation between NDVI and LST (e.g. when NDVI is high the LST is low, therefore high levels of NDVI indicate a high presence of green vegetation). As a result, the high levels of NDVI exist over the western part of the city, e.g. the Sami Abdulalrahman Park. Furthermore, levels of high NDVI could be observed around the city centre in a circular pattern, which indicates the presence of frontal-garden houses (Figures 21 and 22). However, the low levels of NDVI indicate less vegetation in the area, for instance the area is located in the southern part of the city represented by the industrial area, which has the lowest NDVI. The citadel and the commercial surroundings also represent a low level of NDVI due to the commercial aspects of the centre and the central gardens (small size gardens) that dominating the area. Moreover, the houses without gardens observed in the western and some eastern parts of the city. The LULC type of mixed bare soil and houses in the outer eastern part of the city have low levels of NDVI.

There is a polygon in the southern part of the city corresponding to the industrial area of Erbil with high surface temperature. The Industrial part of the city could be noticed to be as a prominent feature of the LST image, due to a sharp contrast between high and low LSTs within the southern part of the city. The city centre as well experience a development of UHIs but less significantly compare to the industrial part. However, pockets of low LSTs could also be observed within the central part of the city due to small parks randomly distributed around the citadel of Erbil. The low LSTs observed as well in the very southern part that corresponded to a green urban area and some houses with frontal gardens. Low LSTs were also observed noticeably over Ainkawa the northern neighborhood of the city, corresponding to frontal-garden houses (LULC type).

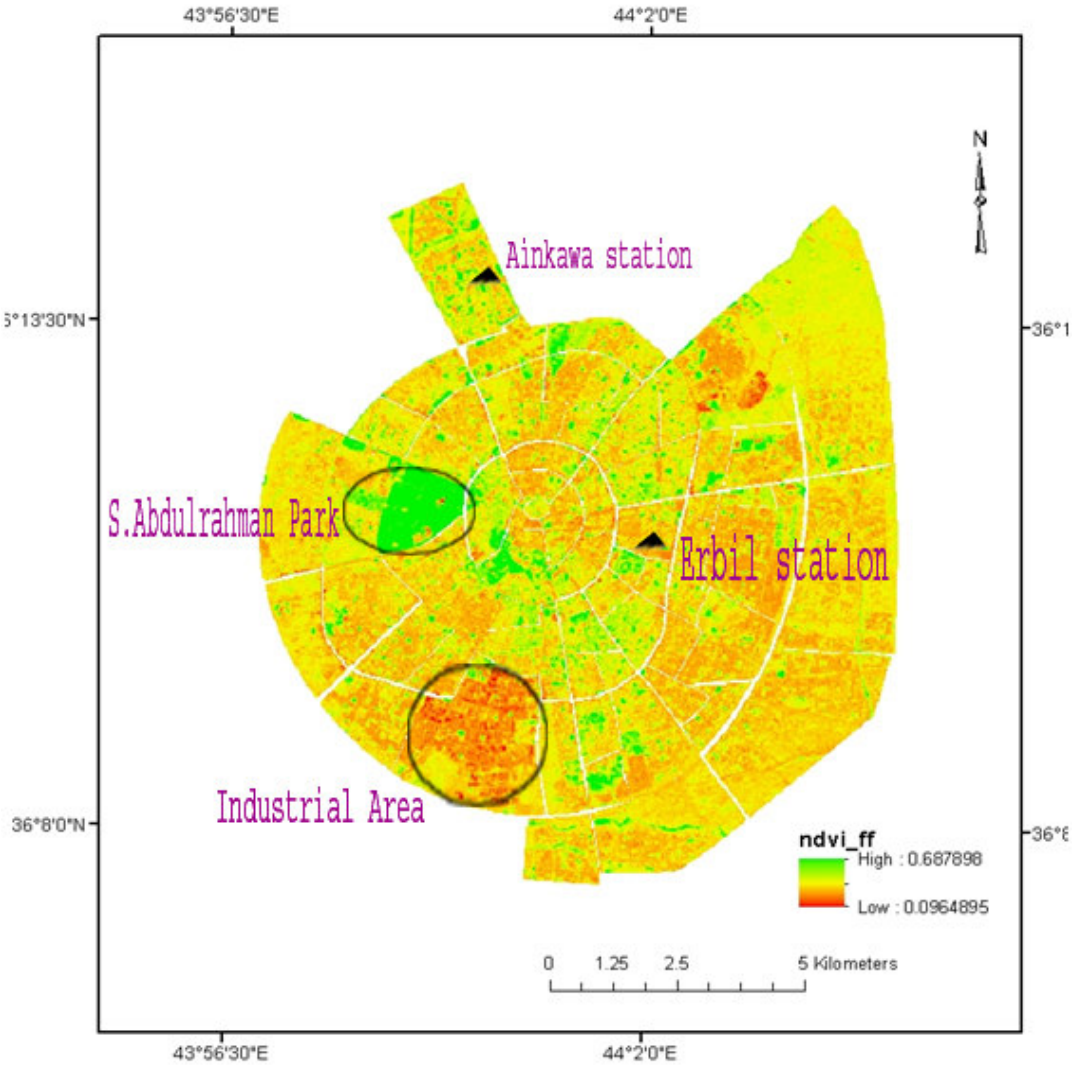

Figure 21: NDVI image of the study area (14 September 2011).

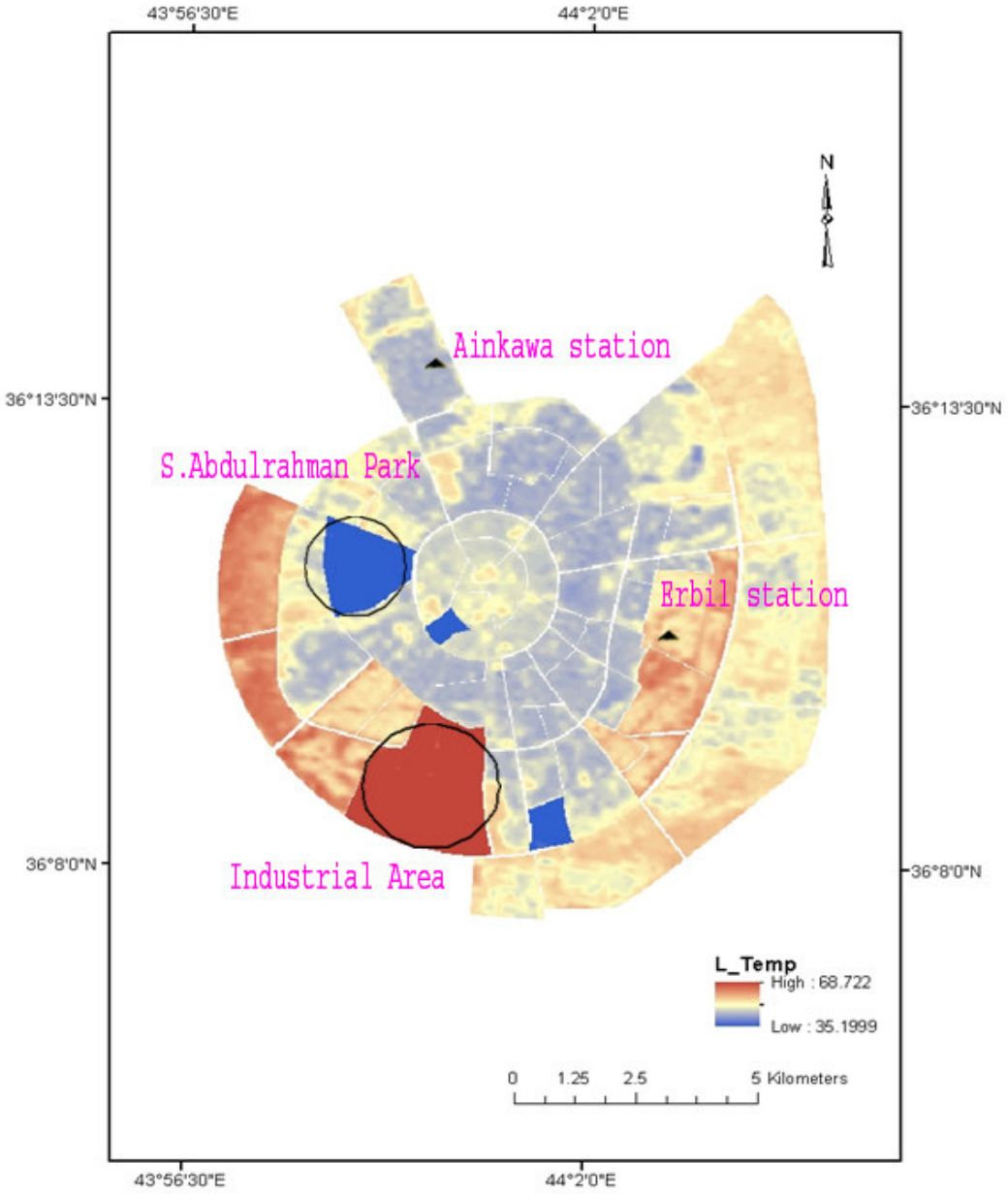

Figure 22: Emissivity corrected LST image of the study area (14 September 2011).

4.2.2 Differences in Mean NDVI and Mean LST

As indicated in the method section the Mean computation of NDVI and LST by the type of LULC were derived using means of a zonal summary GIS operation. The statistical Mean enables a better understanding of the relationship between NDVI, LST and LULC. The GIS zonal statistics results are presented in Figures 23 and 24, depicting the mean NDVI and mean LST for each aggregated LULC type.

The LULC type Park exhibited the highest mean NDVI (0.35) due to the predominance of vegetation within this LULC type. This was followed by the LULC-type houses with frontal gardens, having a value of 0.22. These LULC types also exhibited some of the lowest mean LST values for the study area (40°Cand 47.5°C respectively), which indicates an increased relative rate of evapotranspiration that influence the energy transfer patterns of these LULC types (Wilson et al., 2003).

The LULC type with the lowest mean NDVI value was industrial area (0.18). The LULC type's houses without gardens also show low mean NDVI (0.2). The LULC types of commercial mixed with central gardens houses and bare soil mixed with houses without gardens have an intermediate mean NDVI value compared to the all other LULC types. As stated above, the LULC types with the lowest mean NDVI values exhibited the highest mean LST values, and since there are no water bodies, based on the calculated emissivity all the LULC types with low mean NDVI have a high mean of LST values and vice-versa.

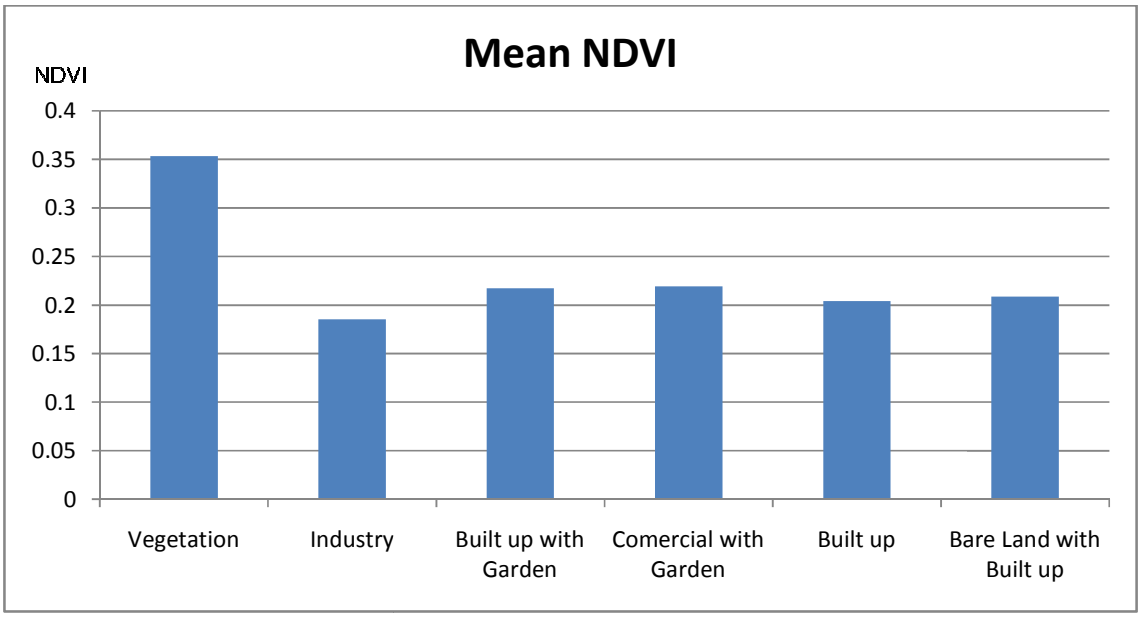

Figure 23: Mean values of NDVI associated with each type of LULC.

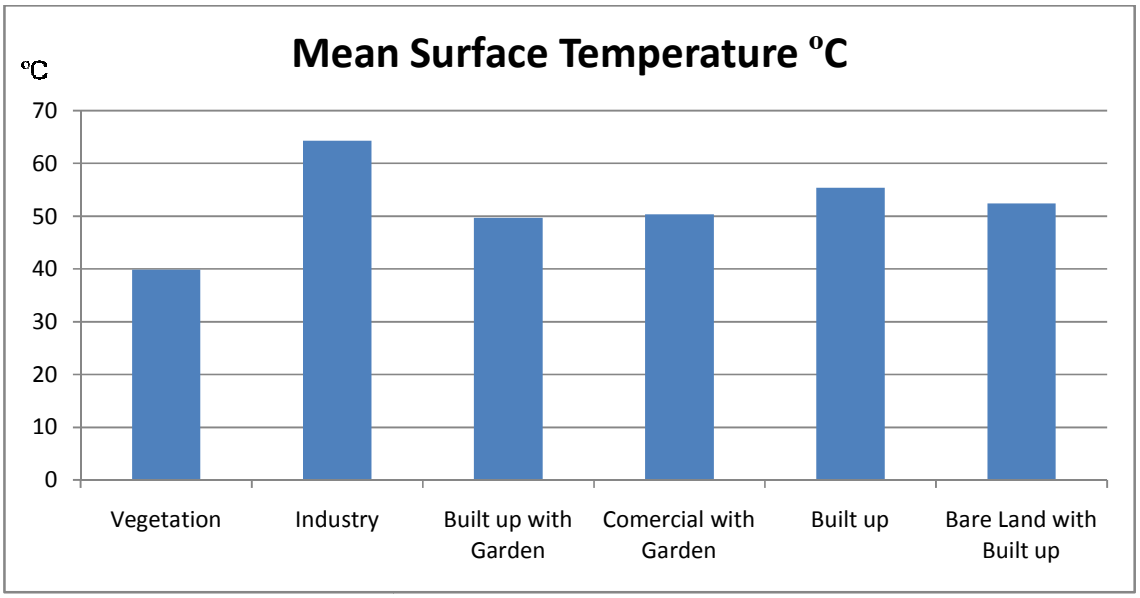

Figure 24: Mean values of LST associated with each type of LULC.

4.2.3 Relationship between NDVI and LST

To better comprehend the relationship between NDVI and LST regression analysis was conducted with the means of each LULC polygon in the study area. The results of the regression analysis are depicted in Figure 25, wherein each point corresponds to the mean value of NDVI and LST. The LULC polygons with low NDVI registered a high LST reading; the LULC polygons with high NDVI generally registered low LST readings.

A significant inverse correlation is evident from the results between NDVI and LST. R-square for the regression is 0.575 indicates that the model explains all the variability of the response data to some extent around its mean.

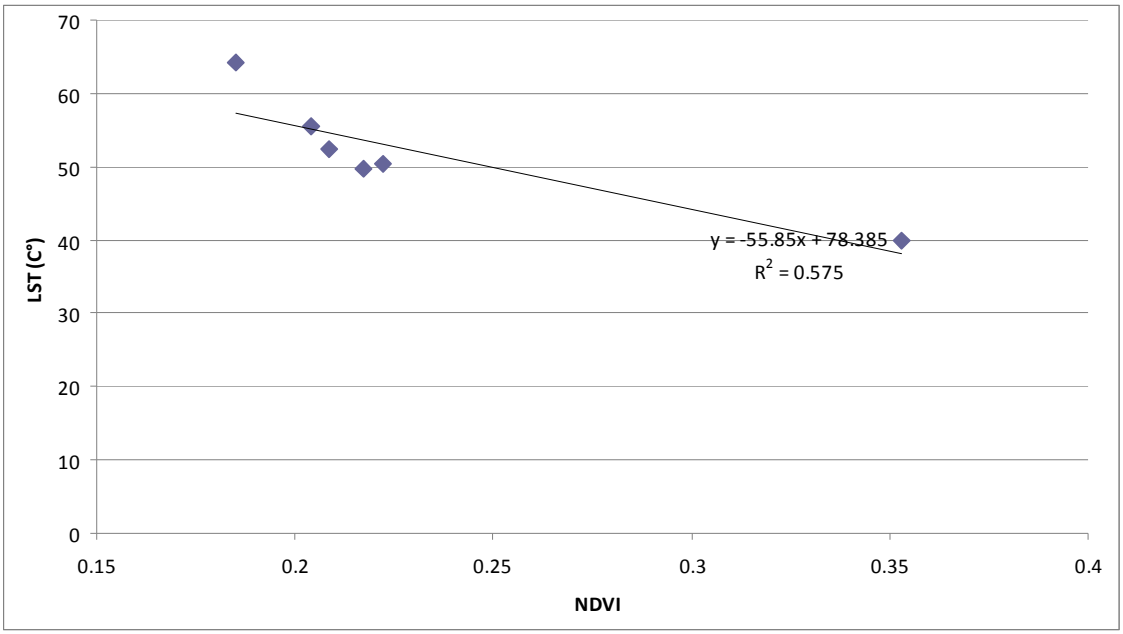

Figure 25: Linear regression scatter plot of mean NDVI and LST associated with every LULC.

5. Discussion and Conclusion

5.1 Discussion

Earth's mean air temperature close to the surface has increased by about 0.8 ℃ since the late of twentieth century; with about two-thirds of the temperature increment was occurring since 1980 (ACC, 2011; Houghton et al., 1990). Earth's mean air temperature increased due to several reasons. These reasons are probably changes in sun intensity, industrial revolution and the global transformation of porous bare and agricultural land to non-permeable urban landscape (IPCC, 2007). The global transformation of porous bare and agricultural land to non-permeable urban landscape is manifest in the built up area of Erbil City, which was anticipated to increase from 45 km^2 in 2001 to 54 km^2 in 2006 and approximately 64 km^2 in 2011 (appendix II).The consequence of the rapid urbanization and other accompanied anthropogenic activities, such as increasing use of air conditioning systems and automobiles in the last decade in the city, have led to the availability of more energy to heat the air.

It was clear from the temporal urban ground weather station measurements and analyses for the period of 1975-2011 that presented a trend toward increasing daily minimum air temperature of about 0.055°C/year, i.e. 1.95 ℃ in 35 years based on monthly averages. In Erbil, there was an increase in annual minimum temperature during the period of 1975-2011 (particularly in the last part of the period 1995-2011 compared to the periods 1975-1990 and 1985-2000). The annual minimum temperature trend incrementing by 0.055 ℃/year is almost in accordance with some studies, for example at an annual level the minimum temperature has incremented by 0.066 ℃/year for the Maxicali urban weather station in a study conducted by García-Cueto, et al (2009). The less differences between the two study results is probably due to the nearly similar climate and rate of urbanization that both area experience. Furthermore, monthly mean minimum and maximum temperatures for about 37% of the global landmass indicate that the rise of the minimum temperature has occurred at a rate of about three times that of the maximum temperature during the period 1951-1990 (Karl, et al 1993). However, in some other studies the maximum and minimum temperatures have witnessed a different trend, for example in India the maximum and minimum temperatures have increased at similar rates, and that is probably because of the study area was located around the tropical zone. (David et al, 1997).

The higher air temperature in the city compared to rural areas is evident in the isotherms of minimum air temperatures (Figures 20). The higher values of minimum temperature, for winter and autumn, are observed in Erbil weather station and Ainkawaw (the nearest weather station to Erbil), which signals the UHI. However, Basotra rural station was also illustrating a warm zone in most seasons for minimum temperature and Kalak for the maximum temperature (Figure, 21). These anomalies might be resulted from the low altitude that these weather stations locate, which is 270 m for Bastora and 250 m for Kalak above sea level, Table 3. The IDW interpolation is easy to apply and has advantage when interpolating the temperature during winter season where our most UHI is expected to occur for small sampled area (Bhowmik, 2012; H. X. Chai et al, 2011). However, Jarvis and Stuart (2001a), state that the elevation emerged as the strongest covariate for both daily minimum and maximum temperature estimating in the IDW interpolation. Regardless of the elevation influence, the few number of stations and their short time period and the increase of discontinuity among the stations are important reasons to reduce the efficiency of the interpolation. Moreover, in order to have better results for the IDW interpolation, there is a need to obtain a dense of station distributed in all directions in the area (Naoum, S. & Tsanis, I.K., 2004).

Based on the emissivity value of each LULC, inverse relationships between vegetation abundance and LST were observed as a whole for the study area. It was clear from the visual interpretation of NDVI and LST that the LULC type green parks and houses with frontal gardens indicate a cold spots on the image due to the abundance of vegetation. However, the industrial area and the houses without gardens had no vegetation, and witness the formation of the hottest spots in the study area, that contributed to the UHI of Erbil.

Erbil has recently been experiencing considerable population growth from 405477 in 1984 to 1,025,000, in 2008 (KRG, 2012). Accordingly, additional residential, industrial and commercial areas are likely will be developed in the near future. It's observed that the UHI is develops more in the downtown (Fortuniak, 2009; Arrau and Pena, 2010). However, in Figure 23, most of the western fringe of the city is warmer, together with parts of the eastern mid-section registering a second high thermal spots to be observed after the industrial area on the map. The reason is the high incident of solar radiation at the surface due to low H/W ratio. Moreover, the less vegetation these areas contain and the existing of no gardens houses might influence the surface temperature. As residential LULC already occupies large portions of the city the thermal characteristics of such LULC could likely have a considerable impact on Erbil thermal environment. It is therefore very necessary for policy makers to decide into

which types of residential houses could be most helpful to be built. The location of industrial area should be taken in consideration if we have to reduce the overall thermal reflection of the city. The thermal reflection reduction might be either by recommending policies for extensive plantation in the area or transfer it out of the city. Furthermore, in order to decrease the urban air temperatures there is a need to dedicate more land for green zones which are disproptionaly distributed in the city.

The thermal image is a good indicator for the variation of surface temperature on the 14th of September 2011. It allows us to identify areas with higher surface temperature and those with lower surface temperature inside the city. The thermal characteristics of each LULC presented in the satellite image depend mainly on the amount of vegetation and the materials used in the process of urbanization (metal and concrete) that have an affective rule on the thermal reflectivity inside Erbil. In addition to the vegetation portions there are several factors affect the surface temperature variation inside the city that should be considered. The type of vegetation whether they are trees, bushes, crops or grasses and the geometry of the surfaces (if they have a high or low H/W ratio). Moreover, in order to obtain more reliable results for the UHI calculation, the SVF is very important factor to be involved (Voogt, 2002; Zhang and Wang, 2008). For example, a larger openness to sky of the canyon namely a high sky view factor leads to more heating during the daytime and faster cooling during the night (Ali-Toudert, F. 2005).

5.2 Conclusion

The replacement of vegetation and open land by urban landscapes and anthropogenic activity tends to be the main factors responsible for the detected changes in the climate patterns and temperature increase of Erbil City. The study included the explanation of the urbanization effect on the local climate of Erbil City based on two sets of data. The first analysis was applied on the data collected from ground weather stations. An urban weather station in Erbil and surrounding rural stations from the year 1975 to 2011 were involved in the study. It was found that Erbil urban weather station showed a tendency of minimum temperature increasing at an annual level rate of 0.055ºC. The months that showed the highest increase in daily minimum temperature were February (0.085ºC/year) and December (0.084ºC/year).

The time series have been divided in three periods; these periods have been decided using the social, political and commercial development of the city as criteria. The findings upon these three periods were significant when comparing the minimum temperature of 1995-2011 periods which witnessed the most intense urban growth with the 1975-1990 and 1985-2000 periods. The ground weather stations were used for spatial analysis of minimum and maximum temperatures; leading to the finding that the highest values are located in the urban zone was obvious during winter and autumn seasons of the year. Generally, Erbil City shows relatively high values of minimum air temperature, followed by Ainkawa, while to the north of the city there are lower readings for the temperature due to the mountainous characteristics of that area. To the west of the city, Kalak weather station recorded low temperatures because of forest availability around the station.

The second analysis of results was presented based on the Satellite Image of Erbil City by extracting the LST based on the emissivity of each LULC. It was concluded from the LST map that generally all the areas with abundant vegetation have lower temperatures than those with no or sparse vegetation. The NDVI and the LST have an inverse relationship, whereby if the LULC has a value of high NDVI the LST is correspondingly low. The fully vegetated LULC represented by parks demonstrated the lowest LST, followed by the LULC type of houses with frontal gardens. On other hand, the LULC of industrial zones exhibited the highest value of LST, followed by the LULC of houses without gardens. These findings comprise a useful case study for those involved in urban and ecological planning in Erbil, particularly for the houses with no gardens which have become a trend for the emergent middle-class inhabitant of Erbil City.

It has been suggested from the results that the urbanization process has led to a warmer micro-climate (mainly the increase of minimum air temperature) in Erbil City compared with its surroundings. Accordingly, policy makers who are interested in planning for future water availability and energy consumption must begin to more carefully recommend the spatial patterns associated with the climate of the growing Erbil City.

References

Akbari, H. (2005). Potentials of Urban Heat Island Mitigation, *International Conference on Passive and Low Energy Cooling for the Built Environment*, Santorini, Greece.

Ali, Toudert and F. Mayer, H. (2005). Thermal comfort in urban streets with trees under hot summer conditions. Proc. 22th Conference on Passive and Low Energy Architecture (PLEA), Beirut, Lebanon. 13-16 Nov. 2005, Vol. 2. pp. 699-704.

America's Climate Choices. Washington, D.C.: The National Academies Press. 2011. p. 15. Available online at: http://www.nap.edu/openbook.php?record_id=12781&page=1

Arnfield J. A. (2003). Two decades of urban climate research: a review of turbulence, exchanges of energy and water, and the urban heat island. *Int. J. Climatol.* 23, 1-26.

Arrau, C. P., and Pena, M. A. (2010). *The Urban Heat Island (UHI) Effect*. Available online at: http://www.urbanheatislands.com [last accessed 25 November 2013].

Artis, D. A. and Carnahan, W. H. (1982). Survey of emissivity variability in thermography of urban areas. *Remote Sensing of Environment*, 12, 313-329.

Ayad, M. Fadhil (2010). Drought Mapping Using Geo-information Technology for Some Sites in the Iraqi Kurdistan Region. International Journal of Digital Earth, Volume 4, Issue 3, 2011, Taylor & Francis.

Balling, C. R. Jr. and Cerveny, R. S. (1987). Long-term associations between wind speeds and the urban heat island of Phoenix, Arizona. *J. Climate Appl. Meteor.* 26, 712-716.

Berdahl, P. and Bretz, S. (1997). Preliminary survey of the solar reflectance of cool roofing materials. *Energy and Buildings* 25 , 149-158.

Bhowmik, Avit K. June 2012. Evaluation of Spatial Interpolation Techniques for Mapping Climate Variables with Low Sample Density. Department of Geology, Lund University, Sweden.

Brazel, A. J., Selover, N., Vose, R. and Heisler, G. (2000). The tale of two climates: Baltimore and Phoenix urban LTER sites. *Clim. Res.* 15, 123-135.

Chapman, D. 2005. It's HOT in the City! Geodate 18(2): 1-4.

Changnon, S. A. (1992). Inadvertent weather modification in urban areas: lessons for global climate change. *Bull. Am. Meteorol. Soc.* 73, 619-627.

Chai, H., Cheng, W., Zhou, C., Chen, X., Ma, X. and Zhao, S. (2011) Analysis and comparison of spatial interpolation methods for temperature data in Xinjiang Uygur Autonomous Region, China. Natural Science, 3, 999-1010. doi: 10.4236/ns.2011.312125.

Jeffrey Chow, Raymond J. Kopp, Paul R. Portney (2003): Energy Resources and Global Development,Science,302,1528-1531,(2003).

Christen, A. and Vogt, R. (2004). Energy and radiation balance of a central European city. *International Journal of Climatology* 24(11), 1395-1421.

Climate (2007). *Köppen Classification*. Available online at: http://www.meteorologyclimate.com/koppenclassification.html [last accessed 25 November 2013].

Comrie A. C. (2000). Mapping a wind-modified urban heat island in Tucson, Arizona (with comments on integrating research and undergraduate learning). *Bull. Am. Meteorol. Soc.* 81, 2417-2431.

Coutts AM, Beringer J, Tapper NJ. (2007). Impact of increasing urban density on local climate: Spatial and temporal variations in the surface energy balance in Melbourne, Australia. Journal of Applied Meteorology and Climatology 46: 477-493.

David R. Easterling, Briony Horton, Philip D. Jones, Thomas C. Peterson, Thomas R. Karl, David E. Parker, M. James Salinger, Vyacheslav Razuvayev, Neil Plummer, Paul Jamason, and Christopher K. Folland .(1997), Maximum and Minimum Temperature Trends for the Globe . Science 18 July 1997: 277 (5324), 364-367. [DOI:10.1126/science.277.5324.364]

Edgerton, D. L. (1996). Should Stochastic or Non-stochastic Exogenous Variables Be Used in Monte Carlo Experiments? Economics Letters, 53, 153-159.

Ed. Hatier (1993). "Acid Rain in Europe". United Nations Environment Programme GRID Arendal. Retrieved 2010-01-31.

EPA (2009a). [Environmental Protection Agency] *Reducing Urban Heat Islands: Compendium of Strategies – Urban Heat Island Basics*. Available online at: http://www.epa.gov/heatisland/resources/pdf/BasicsCompendium.pdf [last accessed 25 November 2013].

EPA (2005a). [Environmental Protection Agency]. Cool Pavement Report: EPA Cool Pavements Study, Task 5. Cambridge Systematics, Inc., Chevy Chase, Maryland, 2005.

EPA (2007), [Environmental Protection Agency]. Heat Island Effect. Washington D.C. [http://www.epa.gov/heatisland.html].

EPA (2009b). [Environmental Protection Agency]. *Heat Island Effect*. Available online at: http://www.epa.gov/heatisland/about/index.html [last accessed 25 October 2013].

EPA (2009c). [Environmental Protection Agency]. *Reducing Urban Heat Islands: Compendium of Strategies – Trees and Vegetation*. Available online at: http://www.epa.gov/heatisland/resources/pdf/TreesandVegCompendium.pdf [last accessed 25 November 2013].

Erik Johansson (2006). Influence of urban geometry on outdoor thermal comfort in a hot dry climate: A study in Fez, Morocco, Building and Environment, Volume 41, Issue 10, October 2006, Pages 1326-1338, ISSN 0360-1323.

Eriksonn, T. S., Granquist C, G., 1982, Radiative cooling computed for model atmospheres. Applied Optics Vol.21 No. 23.

Fortuniak, K (2009). Global environmental change and urban climate in Central European cities. International Conference on Climate Change, the environmental and socio-economic response in the southern Baltic region. Szczecin, Poland.

Gaffin R. S., Rosenzweig, C., Khanbilvardi, R., Parshall, L., Mahani, S., Glickman, H., Goldberg, R., Blake, R., Slosberg, R. B. and Hillel, D. (2008). Variations in New York City's urban heat island strength over time and space. *Theor. Appl. Climatol.* 94, 1-11.

Garcia Cueto, O. R., Tejeda Martinez, A., Bojorquez Morales, G. Urbanization Effects Upon The Air Temperature in Mexicali, B. C., MéxicoAtmósfera 2009, 22 (Sin mes) : [Date of reference: 29 / marzo / 2014].

Houghton R.A., G. Marland, J. Hacker, T.A. Boden, et al. (2010). Climate Change, the IPCC (Intergovernmental Panel on Climate Change).

HKO Hong Kong Observatory of HKSAR 2010, http://www.hko.gov.hk/climate_change /climate_change_e.htm).

Huang, J., Akbari, H. and Taha, H. (1990). The wind-shielding and shading effects of trees on residential heating and cooling requirements. *ASHRAE Winter Meeting, American Society of Heating, Refrigerating and Air-Conditioning Engineers*. Atlanta, Georgia.

Watson I.D., G.T. Johnson, Graphical estimation of sky view-factors in urban environments, International Journal of Climatology 7 (1987) 193–197.

Intergovernmental Panel on Climate Change Special Report on Emissions Scenarios (IPCC SRES), 2001. http://www.grida.no/ climate/ipcc/emission.

Intergovernmental Panel on Climate Change (2007). Climate Change 2007: The physical science basis. In Solomon, S., Qin, D., Manning, M., Chen, Z., Marquis, M., Averyt, K. B., Tignor, M. and Miller, H. L. (Eds.) *Contribution of Working Group I to the Fourth Assessment Report of the Intergovernmental Panel on Climate Change*. Cambridge, UK: Cambridge University Press.

IOM International Organization for Migration (2008), Available online at: https://www.iom.int/cms/en/sites/iom/home.html.

Jarvis, C.H. and N. Stuart, 2001a: A comparison among strategies for interpolating maximum and minimum daily air temperatures. Part I: The selection of "guiding topographic and land cover variables, J. Appl. Meteorol. 40, 1060-1074.

Kalkstein, L. S. and Smoyer, K. E.(1993). The impact of climate change on human health: some international implications. *Experientia* 49, 969-979.

Karl T. R., Díaz, H. F. and Kukla, G. (1988). Urbanization: its detection and effect in the United States' Climate Record. *J. Clim.* 1, 1099-1123.

Karl, Thomas R.; Jones, Philip D.; Knight, Richard W.; Kukla, George; Plummer, Neil; Razuvayev, Vyacheslav; Gallo, Kevin P.; Lindseay, Janette; Charlson, Robert J.; and Peterson, Thomas C., "Asymmetric Trends of Daily Maximum and Minimum Temperature" (1993). Papers in Natural Resources. Paper 185. http://digitalcommons.unl.edu/natrespapers/185.

Klysik, K. and Fortuniak, K. (1999). Temporal and spatial characteristics of the urban heat island of Lodz, Poland. *Atmosph. Environ.* 33, 3885-3895.

Landsat Project Science Office(2001). *Landsat 7 Science Data User's Handbook*.Goddard Space Flight Center. Available online at: http://Landsathandbook.gsfc.nasa.gov/handbook/handbook_htmls/chapter11/chapter11.html[last accessed 25 November 2013].

Landsberg, H. E.(1975). Atmospheric changes in a growing community. *Inst. Fluid Dynamics Appl. Math.* Note No. BN 823. College Park, Ma: University of Maryland, 54.

Le Treut H., Somerville R., Cubasch U., Ding Y., Mauritzen C., Mokssit A., Peterson T. and Prather M. (2007). Historical overview of climate change science. In: Climate change 2007: The physical science basis. Contribution of Working Group I to the Fourth Assessment Report of the Intergovernmental Panel on Climate Change.

Liu, K. and Baskaran, B. (2003). Thermal performance of green roofs through field evaluation.*National Research Council of Canada*, 46412.

Lo, C. P, Quattrochi, D. A. and Luvall, J. C.(1997). Application of high-resolution thermal infrared remote sensing and GIS to assess the urban heat island effect. *International Journal of Remote Sensing*, 18, 287-304.

Meyer, W. (1991). Urban heat island and urban health: early American perspectives. *Professional Geographer* 43(1), 38-48

Ministry of Agriculture (2012). Minister of Agriculture and Water Resources meets British Trade and Investment Minister on London and Belfast visit. Available online at: http://www.hawlergov.org/en/article.php?id=1345008533.

NASA (2010). The Enhanced Thematic Mapper Plus. Available online at: http://Landsat.gsfc.nasa.gov/about/etm+.html [last accessed 25 November 2013].

Naoum, S. & Tsanis, I.K. 2004, 'Ranking Spatial Interpolation Techniques Using a GIS-Based DSS', Global Nest: the Int. J., vol. 6, no.1, pp. 1-20.

Oke, T.R., 1973. City size and the Urban Heat Island. Atmospheric Environment 7: 769-779.

Oke, T. R.(1982). The energetic basis of the urban heat island, TR Quarterly Journal of the Royal Meteorological Society 108 (455), 1-24.

Oke, T. R.(1987). Boundary Layer Climates. London: Routledge.

Oke T. R., Johnson, G. T., Steyn,D. G. and Watson, I. D. (1991). Simulation of surface urban heat islands under ideal conditions at night part 2: diagnosis of causation. *Bound. Lay. Meteorol.* 56, 339-358.

Rose, L. A. and Devadas, M. D. (2009). Analysis of surface temperature and land use/land cover types using remote sensing imagery – a case in Chennai City, India. *Seventh International Conference on Urban Climate*, Yokohama, Japan.

Sailor, D.J., Elley, T.B., Gibson, M., 2012. "Exploring the building energy performance of green roof design decisions – a modeling study of buildings in four distinct climates," J. Building Physics, 35 (4), 372-391.

Salahuddin, Y. B., Ahmad, S. H. and Ismail, S. T. (2010). Modernization theory and house garden transformation: a case study in Erbil City. *Journal of Human Settlements* 2(1).

Santana, L. M (2007). Landsat ETM+ image applications to extract information for environmental planning in a Colombian city. *International Journal of Remote Sensing*, 28, 4225-4242.

Schmugge, T., S.J. Hook, and C. Coll (1998), Recovering surface temperature and emissivity from thermal infrared multispectral data, Remote Sensing of Environment, 65:121-131.

Serra, P. J. A. (2007). Estudio de la isla de calor en la ciudad de Ibiza. *Inv. Geogr.* 44, 55-73.

Siegel, S.(1956). *Non-Parametric Statistics*. London: McGraw-Hill.

Sobrino, J. A., Caselles, V.and Becker, F (1990). Significance of the remotely sensed thermal infrared measurements obtained over a citrus orchard. *ISPRS Journal of Photogrammetry and Remote Sensing* 44(6), 343–354.

Stathopoulou, M., Cartalis, C. and Andritsos, A.(2005). Assessing the thermal environment of major cities in Greece. *International Conference on Passive and Low Energy Cooling for the Built Environment*, Santorini, Greece.

Stathopoulou, M., Cartalis, C. and Petrakis, M.(2007). Integrating Corine Land Cover data and Landsat TM for surface emissivity definition: application to the urban area of Athens, Greece. *International Journal of Remote Sensing* 28, 3291-3304.

UNESCO (2010). Available online at: http://*en.unesco.org.*

USGS (2010b). *New Earth Explorer.* Available online at: http://edcsns17.cr.usgs.gov/NewEarthExplorer/ [last accessed 25 November 2013].

Vandermeulen, Valerie; Verspecht, A., Vermeire, B., Van Huylenbroeck, G., Gellynck, X. (November 30, 2011). "The use of economic valuation to create public support for green infrastructure investments in urban areas". Landscape and Urban Planning 103 (2): 198–206.

Voogt, J., 2004. Urban Heat Islands: Hotter Cities. American Institute of Biological Sciences, Washington D.C.

Voogt, A. J. and Oke, T. R. (2003). Thermal remote sensing of urban climates. *Rem. Sens. Environ.* 86, 370-384.

Voogt A. J.(2002). Urban heat island: causes and consequences of global environmental change. In Douglas, I. (Ed.) *Encyclopedia of Global Environmental Change*. Chichester, West Sussex: John Wiley and Sons, Ltd.,vol. 3, 60-66.

Weather Underground(2010). *Weather History.* Available online at: http://www.wunderground.com/history/airport/LEZL/2003/5/18/DailyHistory.html [last accessed 25 November 2013].

Weng, Q.(2003). Fractal analysis of satellite-detected urban heat island effect. *Photogram. Eng. Rem. Sens.* 69, 555-566.

Wilson, J. S., Clay, M., Martin, E., Stuckey, D. and Vedder-Risch, K.(2003). Evaluating environmental influences of zoning in urban ecosystems with remote sensing. Remote Sensing of Environment 86, 303-321.

Huang Y.J., Akbari, H., Taha H. and Rosenfeld A.H. The Potential of Vegetation in Reducing the Cooling loads in Residential Buildings. Journal of Climate and Applied Meteorology. 26 (1987)1103-1116.

Yuan, F. and Bauer, M. E.(2007). Comparison of impervious surface area and normalized difference vegetation index as indicators of surface urban heat island effects in Landsat imagery. *Remote Sensing of Environment* 106, 375-386.

Zhang J. and Y. Wang, 2008. Study of the relationships between the spatial extent of surface heat urban heat islands and urban characteristic factors based on landsat ETM+ data. Sensors 8, 7453-7468.

Zhang, J., Heng, C. K., Malone-Lee, L. C., Hi, D. J. C., Janssen, P., Leung, K. S. and Tan, B. K. (2012), Evaluating environmental implications of density: A comparative case study on the relationship between density, urban block typology and sky exposure. Automation in Construction 22, 90-101. Available online at: http://www.sciencedirect.com/science/article/pii/S0926580511001233 [last accessed 25 October 2013].

Appendix I: Descriptive statistics of the time series of maximum temperature ($T_{a,max}$) at Erbil urban (1975-2011)

Month	Z_1	Z_2	$T_{a,max,\ ^oC}$	std	K.T	R^2	b
Jan	0.77	1.5	12.6	2.4	0.22	0.25	0.025
Feb	-0.84	-0.34	12.9	2.7	0.47	0.34	0.05
March	0.45	0.37	18.8	2.5	0.22	0.35	0.0077
April	0.34	0.15	26.2	3.4	0.17	0.47	-0.027
May	0.25	0.54	31.9	1.5	0.51	0.24	0.045
June	-0.05	-0.64	38.5	2.2	0.27	0.17	0.047
July	0.58	0.53	43.4	1.4	0.34	0.25	0.040
Aug	-0.27	-0.07	43.5	2	0.25	0.45	0.0025
Sep	0.25	-0.05	37	1.7	0.40	0.37	0.005
Oct	0.65	-0.27	30.5	2.4	0.35	0.24	0.0042
Nov	-0.46	-1.25	21.2	1.5	0.52	0.35	–0.052
Dec	-0.91	-0.34	19.5	1.47	0.37	0.55	0.004
Annual			28.5				0.0158

Descriptive statistics of the time series of mean maximum air temperature ($T_{a,min}$) at Erbil urban (1975-2011), where std is the standard deviation, z_1 is the skewness, z_2 is the kurtosis, $R_2$is the regression determination coefficient, K.T is a Kendall-t non-parametric correlation coefficient, and b is the slope of the regression line.

Appendix II: Erbil City built area, classified using IDRISI (Silva)

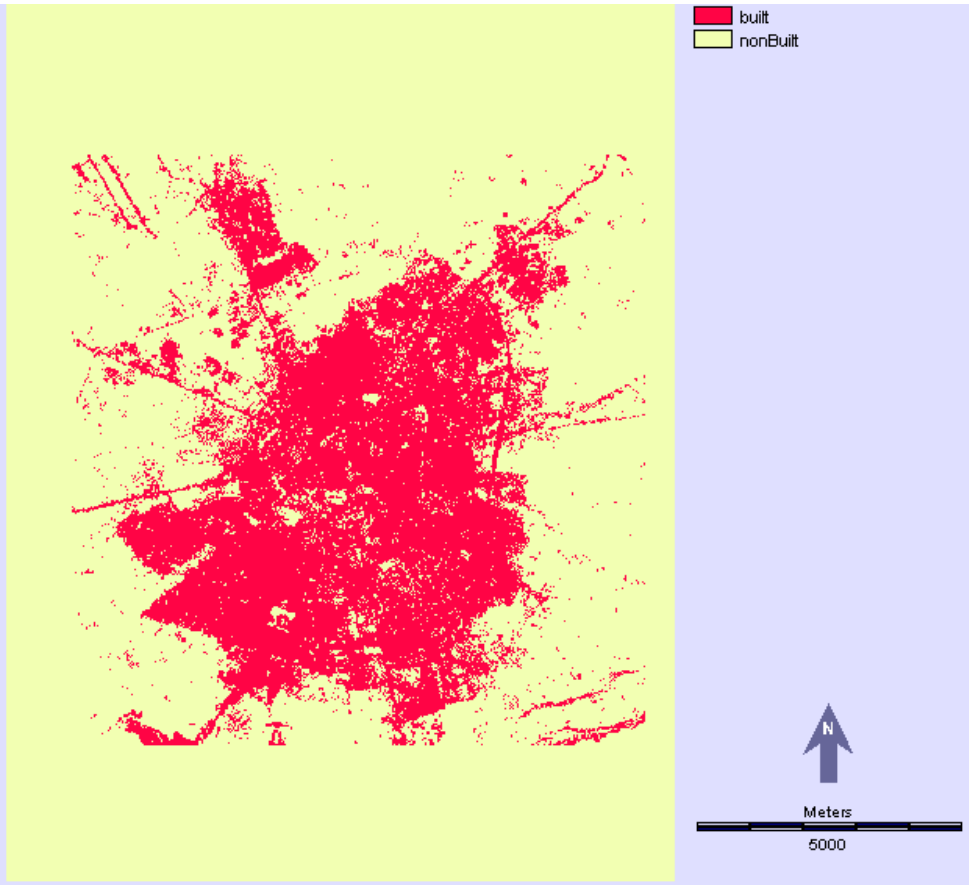

Year: 2000

Category	Square Kilometers	Legend
1	45.3176000	built
2	108438.3873000	nonBuilt

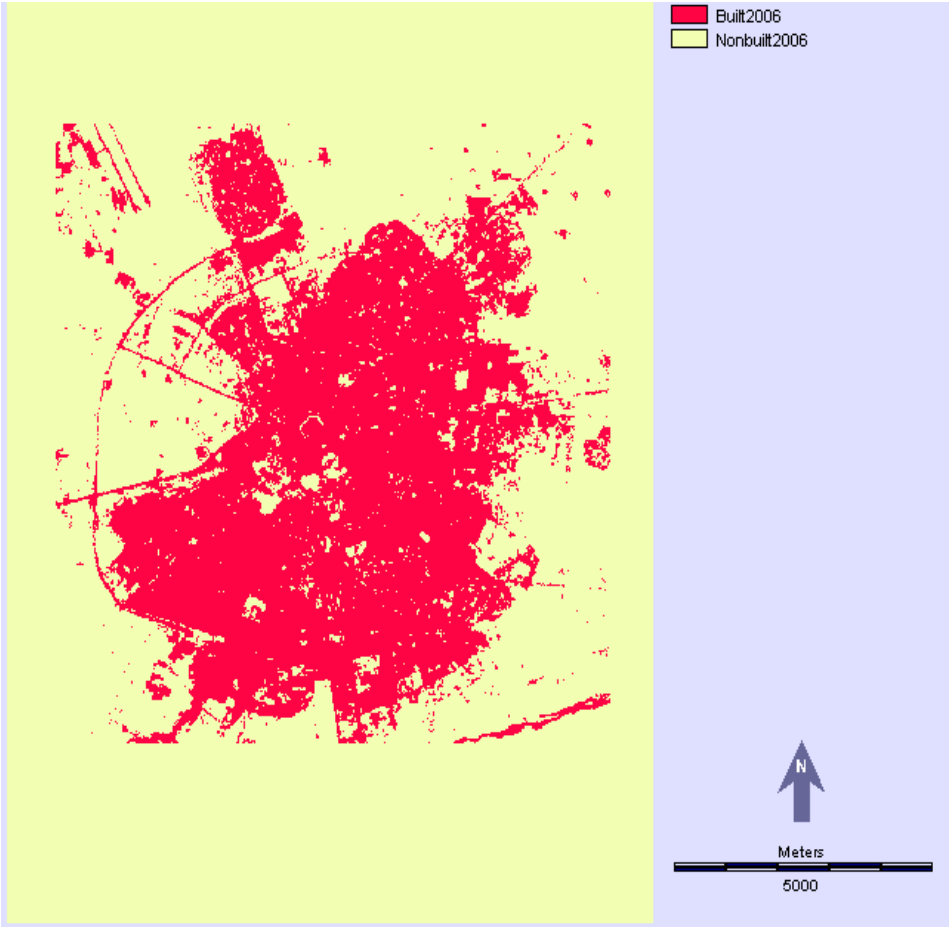

Year: 2006

Category	Square Kilometers	Legend
1	54.1782000	built2006
2	108430.5267000	nonbuilt2006

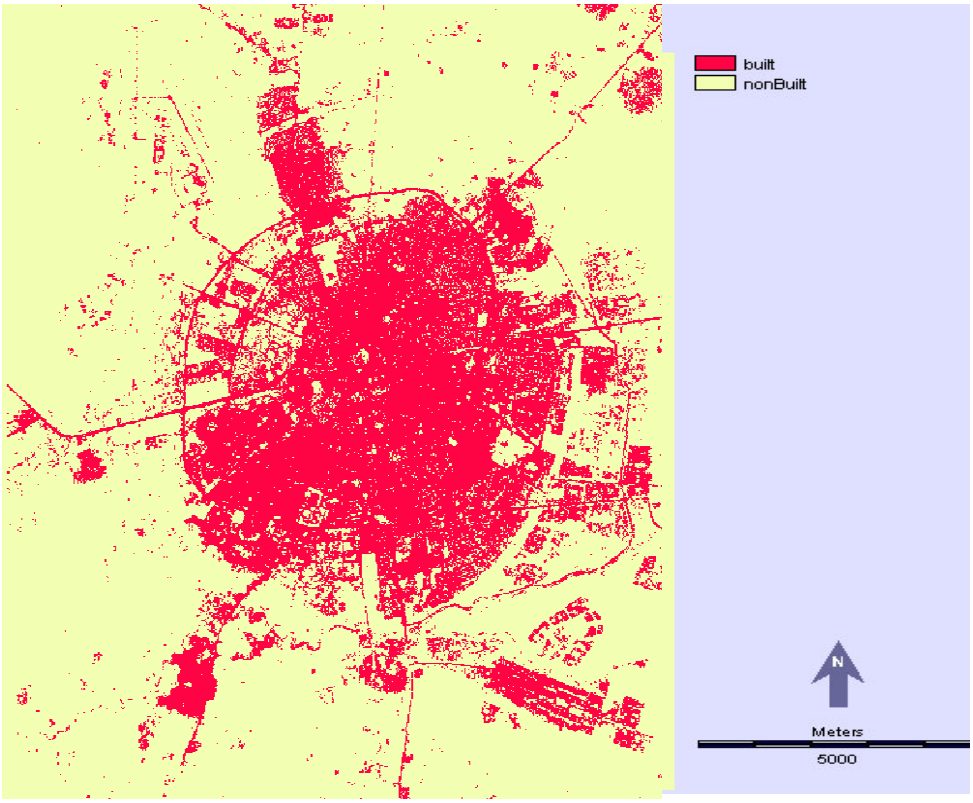

Year: 2011

Category	Square Kilometers	Legend
1	64.31755	built
2	108438.3873000	nonBuilt

Appendix III: Differences in average monthly minimum air temperature between Erbil urban and those selected in the rural between 1985 and 2011 as a graph.

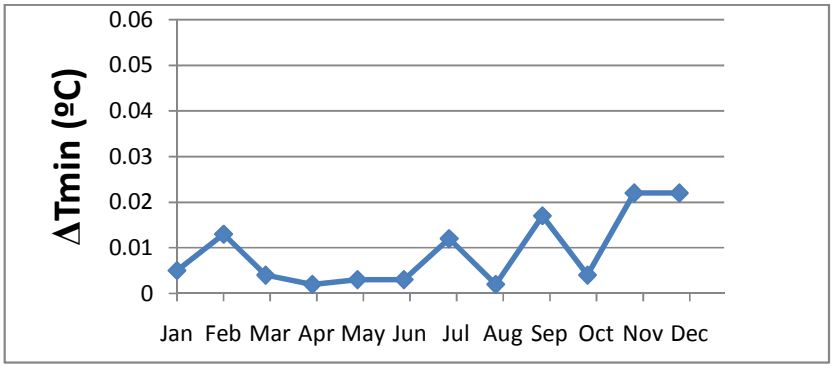

Erbil - Ainkawa

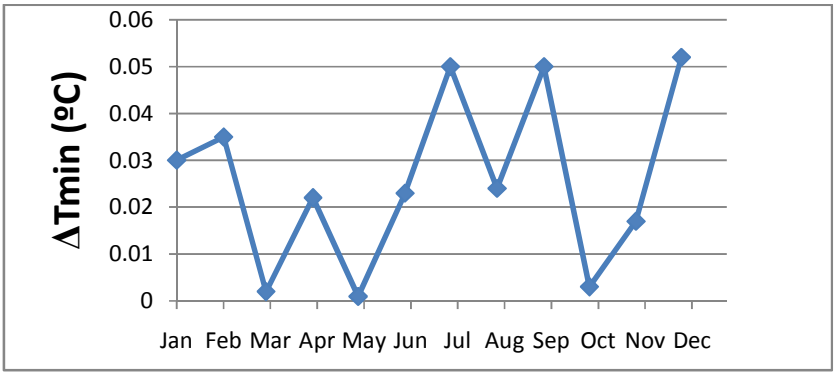

Erbil - Kardarash

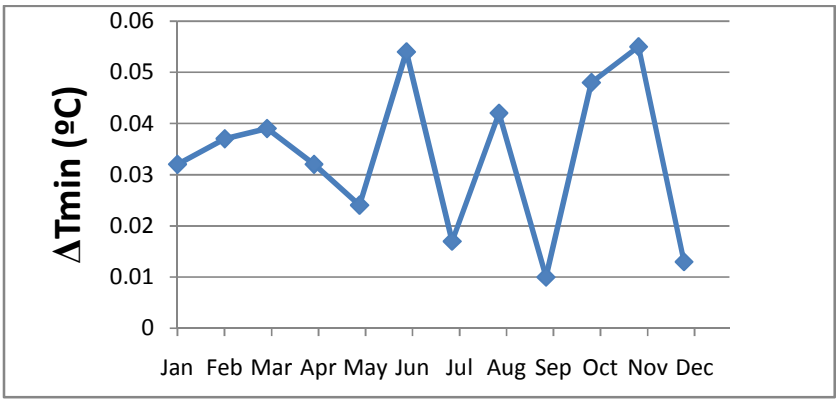

Erbil – Kalak.

Seminar Series,

Institutionen för naturgeografi och ekosystemvetenskap, Lunds Universitet.

Student examensarbete (Seminarieuppsatser). Uppsatserna finns tillgängliga på institutionens geobibliotek, Sölvegatan 12, 223 62 LUND. Serien startade 1985. Hela listan och själva uppsatserna är även tillgängliga på LUP student papers (www.nateko.lu.se/masterthesis) och via Geobiblioteket (www.geobib.lu.se)

The student thesis reports are available at the Geo-Library, Department of Physical Geography and Ecosystem Science, University of Lund, Sölvegatan 12, S-223 62 Lund, Sweden. Report series started 1985. The complete list and electronic versions are also electronic available at the LUP student papers (www.nateko.lu.se/masterthesis) and through the Geo-library (www.geobib.lu.se)

268 Ylva Persson (2013) Refining fuel loads in LPJ-GUESS-SPITFIRE for wet-dry areas - with an emphasis on Kruger National Park in South Africa

269 Md. Ahsan Mozaffar (2013) Biogenic volatile organic compound emissions from Willow trees

270 Lingrui Qi (2013) Urban land expansion model based on SLEUTH, a case study in Dongguan City, China

271 Hasan Mohammed Hameed (2013) Water harvesting in Erbil Governorate, Kurdistan region, Iraq - Detection of suitable sites by using Geographic Information System and Remote Sensing

272 Fredrik Alström (2013) Effekter av en havsnivåhöjning kring Falsterbohalvön.

273 Lovisa Dahlquist (2013) Miljöeffekter av jordbruksinvesteringar i Etiopien

274 Sebastian Andersson Hylander (2013) Ekosystemtjänster i svenska agroforestrysystem

275 Vlad Pirvulescu (2013) Application of the eddy-covariance method under the canopy at a boreal forest site in central Sweden

276 Malin Broberg (2013) Emissions of biogenic volatile organic compounds in a Salix biofuel plantation – field study in Grästorp (Sweden)

277 Linn Renström (2013) Flygbildsbaserad förändringsstudie inom skyddszoner längs vattendrag

278 Josefin Methi Sundell (2013) Skötseleffekter av miljöersättningen för natur- och

kulturmiljöer i odlingslandskapets småbiotoper

279 Kristín Agustsdottír (2013) Fishing from Space: Mackerel fishing in Icelandic waters and correlation with satellite variables

280 Cristián Escobar Avaria (2013) Simulating current regional pattern and composition of Chilean native forests using a dynamic ecosystem model

281 Martin Nilsson (2013) Comparison of MODIS-Algorithms for Estimating Gross Primary Production from Satellite Data in semi-arid Africa

282 Victor Strevens Bolmgren (2013) The Road to Happiness – A Spatial Study of Accessibility and Well-Being in Hambantota, Sri Lanka

283 Amelie Lindgren (2013) Spatiotemporal variations of net methane emissions and its causes across an ombrotrophic peatland - A site study from Southern Sweden

284 Elisabeth Vogel (2013) The temporal and spatial variability of soil respiration in boreal forests - A case study of Norunda forest, Central Sweden

285 Cansu Karsili (2013) Calculation of past and present water availability in the Mediterranean region and future estimates according to the Thornthwaite water-balance model

286 Elise Palm (2013) Finding a method for simplified biomass measurements on Sahelian grasslands

287 Manon Marcon (2013) Analysis of biodiversity spatial patterns across multiple taxa, in Sweden

288 Emma Li Johansson (2013) A multi-scale analysis of biofuel-related land acquisitions in Tanzania - with focus on Sweden as an investor

289 Dipa Paul Chowdhury (2013) Centennial and Millennial climate-carbon cycle feedback analysis for future anthropogenic climate change

290 Zhiyong Qi (2013) Geovisualization using HTML5 - A case study to improve animations of historical geographic data

291 Boyi Jiang (2013) GIS-based time series study of soil erosion risk using the Revised Universal Soil Loss Equation (RUSLE) model in a micro-catchment on Mount Elgon, Uganda

292 Sabina Berntsson & Josefin Winberg (2013) The influence of water availability on land cover and tree functionality in a small-holder farming system. A minor field study in Trans Nzoia County, NW Kenya

293 Camilla Blixt (2013) Vattenkvalitet - En fältstudie av skånska Säbybäcken

294 Mattias Spångmyr (2014) Development of an Open-Source Mobile Application for

Emergency Data Collection

295 Hammad Javid (2013) Snowmelt and Runoff Assessment of Talas River Basin Using Remote Sensing Approach

296 Kirstine Skov (2014) Spatiotemporal variability in methane emission from an Arctic fen over a growing season – dynamics and driving factors

297 Sandra Persson (2014) Estimating leaf area index from satellite data in deciduous forests of southern Sweden

298 Ludvig Forslund (2014) Using digital repeat photography for monitoring the regrowth of a clear-cut area

299 Julia Jacobsson (2014) The Suitability of Using Landsat TM-5 Images for Estimating Chromophoric Dissolved Organic Matter in Subarctic Lakes

300 Johan Westin (2014) Remote sensing of deforestation along the trans-Amazonian highway

301 Sean Demet (2014) Modeling the evolution of wildfire: an analysis of short term wildfire events and their relationship to meteorological variables

302 Madelene Holmblad (2014). How does urban discharge affect a lake in a recreational area in central Sweden? – A comparison of metals in the sediments of three similar lakes

303 Sohidul Islam (2014) The effect of the freshwater-sea transition on short-term dissolved organic carbon bio-reactivity: the case of Baltic Sea river mouths

304 Mozafar Veysipanah (2014) Polynomial trends of vegetation phenology in Sahelian to equatorial Africa using remotely sensed time series from 1983 to 2005

305 Natalia Kelbus (2014) Is there new particle formation in the marine boundary layer of the North Sea?

306 Zhanzhang Cai (2014) Modelling methane emissions from Arctic tundra wetlands: effects of fractional wetland maps

307 Erica Perming (2014) Paddy and banana cultivation in Sri Lanka - A study analysing the farmers' constraints in agriculture with focus on Sooriyawewa D.S. division

308 Nazar Jameel Khalid (2014) Urban Heat Island in Erbil City.